# ABSTRACT

Title of Dissertation: INTERROGATING PROTEIN CARGOES OF MDSC-DERIVED EXOSOMES ON THE BASIS OF POST-TRANSLATIONAL MODIFICATIONS.

Sitara Chauhan, Doctor of Philosophy, 2017

Dissertation directed by: Dr. Catherine Fenselau, Department of Chemistry and Biochemistry

Myeloid-derived suppressor cells (MDSC) are immature myeloid cells which accumulate in cancer patients and tumor-bearing mice. Their function in the tumor microenvironment is to inactivate the immune response to cancer by suppressing both the adaptive and innate immune system. Therefore, MDSC are a major obstacle in immunotherapeutic approaches designed to cure cancer. MDSC-derived from tumor bearing mice have been found to shed exosomes. Exosomes are nano-sized vesicles that carry biologically active molecules and play a role in intercellular communication. MDSC-derived exosomes have been reported to mediate the immunosuppressive functions of the parental cells by stimulating the accumulation of MDSC and also by converting macrophages to a tumor-promoting phenotype.

Recent developments in government policy have launched a goal of curing cancer using immune-based therapies (Cancer MoonShot 2020). The understanding

of the mechanisms and functions of MDSC immune suppression will be crucial in the success of these therapeutic endeavors. Our current study focuses on interrogating the protein cargo carried by MDSC-derived exosomes based on differential post-translational modifications (PTMs). Post-translational modifications have important roles in functions, signaling, location and interactions of proteins. Selecting proteins based on a specific post-translational modification can aid in the identification of low-abundance proteins, which may not be identified in a shotgun proteomics approach.

The first aim of this work was to successfully modify an existing surface chemistry method to use on exosomes. We then used a proteomic strategy to identify glycoproteins on the surface of MDSC-derived exosomes, and then test if selected glycoproteins contribute to exosome-mediated chemotaxis and migration of MDSCs. Furthermore, we also aimed at examining the ubiquitome of the MDSC-derived exosomes, using top-down and bottom-up proteomics. Since inflammation has been reported to enhance the tumor promoting activity of the MDSC, the bottom-up analysis focused on the effects of increased inflammation on the ubiquitination of the protein cargo of MDSC-derived exosomes. Spectral counting was used to estimate differences in abundance of proteins found with ubiquitinated proteoforms in high and basal levels of inflammation. The top-down analysis aimed at characterizing the length and topology of ubiquitin linkages on substrate proteins in MDSC-exosomes.

# INTERROGATING PROTEIN CARGOES OF MDSC-DERIVED EXOSOMES ON THE BASIS OF POST-TRANSLATIONAL MODIFICATIONS

by

Sitara Chauhan

Dissertation submitted to the Faculty of the Graduate School of the
University of Maryland, College Park, in partial fulfillment
of the requirements for the degree of
Doctor of Philosophy
2017

Advisory Committee:
Professor Catherine Fenselau, Chair
Professor Don Milton, Dean's Representative
Associate Professor Jason Kahn
Associate Professor Douglas Julin
Professor Suzanne Ostrand-Rosenberg

# Dedication

*This work is dedicated to my guys David, and Artemus. Thank you for always having my back, urging me forward, loving me fiercely, and making me laugh.*

# Acknowledgements

I would first like to thank my academic advisor Dr. Catherine Fenselau for the guidance she provided me through my graduate studies. Dr. Fenselau taught me how to think about and communicate science, for which I will be forever grateful. She has also imparted important lessons in leadership, time management and organization, which are skills that certify success in every endeavor one sets upon. I would also like to thank Dr. Yan Wang for training provided on several instruments and bioinformatics tools, for always listening to my ideas, having experiment-saving suggestions, and for sometimes reminding me of the bigger picture. I would also like to acknowledge our collaborators: Dr. Suzanne Ostrand-Rosenberg for providing MDSC and MDSC-derived exosome samples and for many discussions on cellular biology and immunology; and Dr. Nathan Edwards for teaching me about bioinformatics. A special acknowledgement to Dr. Marvin Schulte, who encouraged me to study biochemistry and provided guidance through my undergraduate education.

I have had the greatest fortune of being a part of a team of dynamic, talented, and supportive young female scientists. I thank: Dr. Avantika Dhabaria, and Dr. Waeowalee Choksawangkarn for their guidance and training during the first few months of graduate school; Dr. Meghan Burke and Yeji Kim for setting the bar high and exemplifying hard work and dedication; Kate Adams, for teaching me to pay attention to detail; Dr. Lucia Geis for showing me a compassionate approach to working in the lab; thank you for sharing your brilliance and for the invaluable lessons in lab; and Dr. Amanda Lee, for showing me a no-nonsense approach to life,

helping me find the confidence inside me, and for all the laughs we shared. These women have taught me countless lessons in friendship, humility and good teamwork, and I will always look back on the days we worked together as one of the highlights of graduate school. I would also like to acknowledge post-doctoral fellows Dr. Dapeng Chen and Dr. Fabio Gomes for their advice and help.

I would like to acknowledge my graduate school family of friends: Shweta Ganapati, Kim Hyunh, Tessy Thomas, Amanda Lee, Steve Wolf and Marcus Canter, for being my rocks through it all. For always showing up when it mattered and also for showing up when it didn't. Thank you to my biochemistry classmates: Katherine Burgomaster, Bill Cressman, Dulith Abeykoon, Diana Zhang, Hyeyeon Nam and Adam Gamson, for study group sessions and your support as we took on each new challenge together.

Lastly, I would like to thank my parents, Devendra and Rashmi Chauhan, for providing me the opportunities to explore my interests and for their generous support, which allowed me to follow my dreams, and achieve them. I would also like to thank my brother Arsh for his patient help with writing code to make data analysis easier. I'd like to thank my husband David, for inspiring me to be a better person and a better scientist. Thank you for being an equal partner, for editing my work, and most importantly for coffee in the mornings. I would finally like to acknowledge my son Artemus, for bringing me joy, and making me appreciate every new day and the challenges it may bring.

# Table of Contents

# List of Tables

# List of Figures

# List of Abbreviations

| | |
|---|---|
| ACN | Acetonitrile |
| cAMP | Cyclic adenosine monophosphate |
| Cbl-b | Casitas B-lineage lymphoma proto-oncogene B |
| CD | Cluster of differentiation |
| CD11b | Integrin alpha-M |
| CD14 | Myeloid cell-specific leucine-rich glycoprotein |
| CD15 | Fucosyltransferase 9 |
| CD157 | ADP-ribosyl cyclase |
| CD172a | Signal regulatory protein alpha |
| CD321 | Junction adehsion molecule A |
| CD33 | Sialic acid-binding Ig-like lectin 3 |
| CD47 | Leukocyte surface antigen |
| CID | Collision-induced dissociation |
| CON | Conventional |
| CREB | Cyclic adenosine monophosphate response element-binding protein |
| cryo-EM | Cryo-electron microscopy |
| DUBs | Deubiquitinases |
| ESCRT | Endosomal sorting complexes required for transport |
| ETD | Electron tranfer dissociation |
| FDR | False discovery rate |
| FTICR | Fourier transform ion cyclotron resonance mass spectrometry |
| GG | Glycinylglycine |
| GM-CSF | Granulocye-macrophage colony stimulating factor |
| Gr1 | Gamma response 1 |
| GRAIL | Gene related to anergy in lymphocytes |
| HCD | Higher-energy collission dissociation |
| HF | High-field |
| HMGB1 | High mobility group box protein 1 |
| Hsp | Heat shock proteins |
| IAA | Iodoacetamide |
| IL | Interleukin |
| IL-1β | Interlekin-1beta |
| ILVs | Interluminal vesicles |
| INF | Inflammatory |

| | |
|---|---|
| Itch | Itchy E3 ubiquitin protein ligase |
| LC | Liquid Chromatography |
| LFA-1 | Leukocyte function antigen 1 |
| LUBAC | Linear ubiquitin chain assemby complex |
| MDSCs | Myeloid-derived suppressor cells |
| MoaD | Molybdopterin synthase sulfur carrier subunit protein |
| MVBs | Multivesicular bodies |
| NF-kβ | Nuclear factor-kappa-light-chain enchancer of activated B-cells |
| NL | normalized signal intensity |
| PGE2 | Prostaglandin E2 |
| PTM | Post-translational modification |
| RAGE | Receptor for Advanced Glycation Endproducts |
| RIC | Reconstructed ion chromatogram |
| RNA | Ribonucleic acid |
| Rsc | Ratio of spectral counts |
| STAT | Signal tranducer and activator of transcription |
| SUMO | Small ubiquitin-related modifier |
| TCR | T-cell receptor |
| TEM | Transmission electron microscopy |
| Th17 | T cells and T helper 17 |
| ThiS | ThiaminS |
| TME | Tumor microenvironment |
| TSP-1 | Thrombospondin-1 |
| TUBES | Tandem ubiquitin binding entities |
| Ub | Ubiquitin |
| UbiCRest | Ubiquitin chain restriction |
| UbL | Ubiquitin-like proteins |
| UC | Urea containing |
| VEGF | Vascular endothelial growth factor |
| XIC | Extracted ion chromatogram |

# Chapter 1: Introduction

## *1.1. Research significance and objectives*

Exosomes were first discovered in 1983 when transferrin receptors were observed to be leaving reticulocytes on vesicles of ~50 nm in diameter.[1] The field of exosome research has exploded in the last three decades, resulting in over a thousand publications on the topic as scientists try to better understand their role in cellular communication. Exosomes have been found to be generated by both healthy and cancerous eukaryotic cells. In the realm of the tumor microenvironment, most studies have focused on exosomes released by tumor cells. [2–5] However, the tumor microenvironment is also composed of several types of cells that contribute to tumor-induced immune suppression. This study focuses on one of these cellular players: myeloid derived suppressor cells (MDSC) derived exosomes and their role in intercellular communication in the tumor microenvironment. They are immature myeloid cells that accumulate in the tumor microenvironment. MDSC are immunosuppressive cells that aid in tumor progression by suppressing T cell activation and redirecting macrophage polarization towards a tumor promoting type, among other functions.[6] Exosomes shed by MDSC have been found to carry a biologically active cargo of proteins and small RNAs, which contribute to their parental cells' immunosuppressive function.[7]

Exosomes are thought to be players in intercellular communication in that they can transfer their cargo to cells in their environment. Interacting with a recipient cell is thought to involve the binding of a specific exosome receptor to the cell surface followed by endocytosis and fusion.[8] Surface proteins are known to be involved in a host of important functions including adhesion, transport and the provision of receptors for signaling. Exosomes are

enriched in plasma membrane proteins,[9] but to date an inventory of the surface proteome of exosomes has not been carried out. A study of the surface proteome would provide identifications of low abundance proteins and allow us to gain insight into potential players in communication in the tumor microenvironment.

The mechanism of biogenesis of exosomes and the sorting of biological cargo in exosomes is not well understood. A role for ubiquitination in sorting of proteins into exosomes is still disputed and of interest to the scientific community.[10] Ubiquitination is a post-translational modification (PTM) in which the protein ubiquitin is attached to a substrate protein. This PTM can lead to signaling in a host of different pathways including the nuclear factor kappa-light-chain enhancer of activated B-cells (NF-κB) pathway, DNA damage response, immune inflammation response and proteolytic degradation among others.[11] Therefore, targeting and analyzing the ubiquitin proteome (ubiquitome) is expected to provide more insights into the biological relevance of the protein cargo carried by MDSC derived exosomes. Both exosome surface glycoproteins and ubiquitinated proteins are studied here using novel proteomic strategies and state-of-the art mass spectrometry.

### *1.2. Myeloid derived suppressor cells*

Myeloid-derived suppressor cells (MDSC) are immature myeloid cells present in cancer patients. MDSC are characterized by marker proteins cluster of differentiation molecule (CD) 11b (CD11b) and gamma response 1 (Gr1) in mice and by marker proteins CD11b, CD14, CD33, and CD15 in humans. [12] Under normal conditions myeloid cells in bone marrow differentiate into macrophages, dendritic cells, and granulocytes.[13,14] However, in conditions of increased inflammation or cancer, myeloid cells do not differentiate correctly and are instead activated to form MDSC (Figure 1.1). MDSC differentiation in bone marrow

is a result of tumor-released factors including reactive oxidation species, nitric oxide and cytokines. It has also been demonstrated that inflammation leads to an increase in MDSC accumulation and immune suppression function. The proinflammatory cytokines involved in MDSC accumulation include but are not limited to interleukin (IL) 1β (IL-1β), IL-6, and prostaglandin E2 (PGE2).[12] Vascular endothelial growth factor (VEGF) and granulocyte-macrophage colony-stimulating factor (GM-CSF) stimulate angiogenesis, drive tumor growth and are involved in MDSC accumulation. Tumor-secreted soluble factors also disrupt normal cellular functioning by altering activation of transcription factors including signal transducer and activator of transcription (STAT) 1, 3 and 6. [12,14]

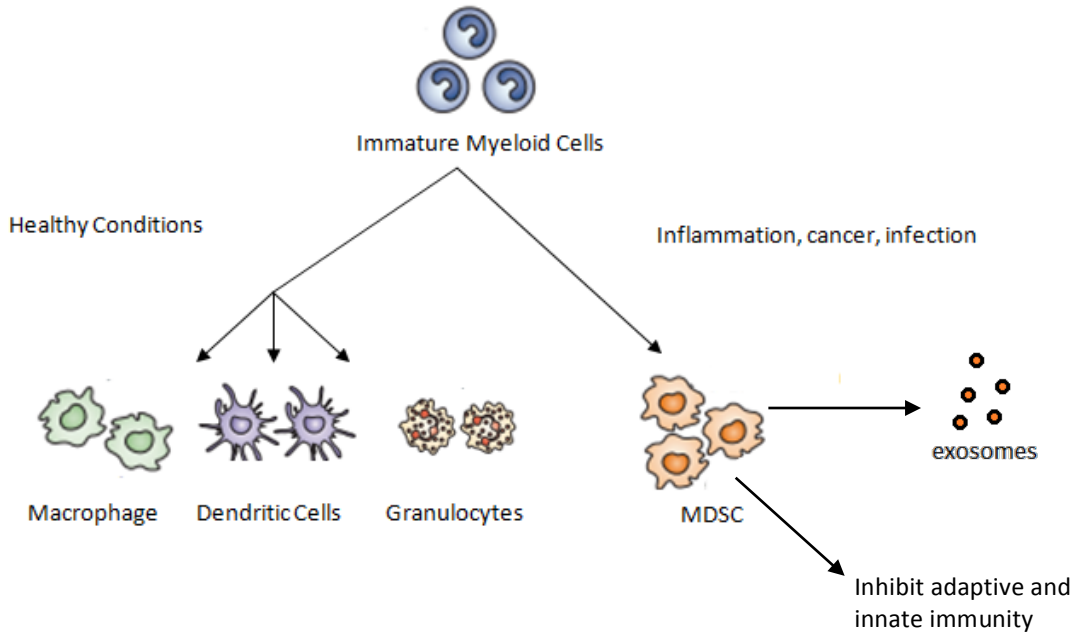


**Figure 1.1.** Depicts the differentiation of immature myeloid cells to form MDSC or other immune cells based on the environment. Adapted from reference 14.

MDSC's role in the tumor microenvironment is that of suppressing the adaptive and innate immune system. The MDSC target T cells and natural killer cells and suppress their activity to promote the growth of the tumor. The mechanisms of their suppressive activity includes the increased production of reactive oxygen species, peroxynitrite release, enhanced

L-arginine catabolism which leads to amino acid starvation, induction of regulatory T cells and T helper 17 (Th17) cells, and induction of apoptosis.[14,15]

A limited number of proteomics studies have been performed on MDSC. Boutte *et al.* compared the proteomes of MDSC from metastatic (murine mammary carcinoma 4T1) and non- metastatic (murine mamary carcinoma 67NR) tumors in mice. [16] Ninety-three percent of the proteins identified in this study were shared between the two types of MDSC, and the study found that the proteins in pathways involved in γ -glutamyl transferase, glutathione synthase and cyclic adenosine monophosphate (cAMP) response element-binding protein (CREB) transcription factor signaling were up-regulated in 4T1 metastatic MDSC.[16] A proteomic study by Chornoguz et al. studied the effect of increased inflammation on the proteomes of 4T1 MDSC in mice. The 4T1 cells were stably transfected with IL-1β, a cytokine that increases inflammation. This study determined that Fas-induced apoptosis, TGF- cytokines, and caspase network stress associated pathways were up regulated in inflammatory MDSC.[17]

Other studies have focused on understanding the role of proteins identified in MDSC. A study by Sinha et al. focused on the role of pro-inflammatory cytokines S100 calcium binding protein A8 (S100A8) and S100A9, which are found in the tumor microenvironment, and their role in MDSC function. MDSC have carboxylated N-glycans on their surface, which serve as receptors for S100A8 and S100A9. MDSC were also found to secrete S100A8/A9 and activate the inflammatory NF-κβ pathway. In addition this study also determined that S100A8/A9 are chemotactic for MDSC, which leads to maintenance of a pro-inflammatory tumor environment.[18] Several proteoforms of S100A8/A9 have been identified using top-down proteomics studies in exosomes shed by 4T1-IL1β.[19,20] Another protein of importance discovered in MDSC is high mobility group box protein 1 (HMGB1). Parker et al. found evidence for the participation of HMGB1 in development of MDSC in bone marrow

progenitor cells. HMGB1 also plays a role in the functions of MDSC and not just in the activation of the MDSC. The protein was found to suppress anti-tumor immunity by suppressing antigen driven T-cell activation. It was also found to increase production of 1L-10, which also drives MDSC-macrophage cross talk. Somewhat surprisingly, HMGB1 was also found to have some anti-tumor activity due to its ability to activate tumor-reactive T cells.[21]

### *1.3. Exosomes shed by myeloid derived suppressor cells*

Exosomes are membrane bound extracellular vesicles, 30-100nm in size. They are shed from all eukaryotic and many bacteria cells. They are different from microvesicles, oncosomes and apoptotic bodies not just in size but also in the method of biogenesis.[22] Exosomes are formed by the inward budding of the plasma membrane to form multivesicular bodies (MVBs). The membrane of the multivesicular bodies buds inwardly and forms interlumenal vesicles (ILVs).[23–25] The formation of the ILV's is still not well understood and is thought to occur by two possible pathways; endosomal sorting complexes required for transport (ESCRT) dependent and ESCRT independent.[26,27] ESCRT proteins such as Alix, and Hepatocyte growth factor–associated tyrosine kinase (Hrs), are shown to be involved in sorting of proteins into exosomes.[28,29] The ESCRT independent pathway relies on sphingomyelinase, an enzyme which produces ceramide.[27] The presence of high ceramide levels in exosomes from oligodendroglial cells and B cells supports this theory.[27,30] Depleting the ESCRT complex has been shown to allow in the successful formation of MVBs.[31]

There are two possible fates of the MVB's: (1) degradation of the MVBs by the lysosome, or (2) release of the ILV's into the extracellular milieu, where they are classified as exosomes (Figure 1.2).[32] Larger vesicles and cell debris are first removed from the cell

culture with low speed centrifugation. Extracellular vesicles are then isolated from biological fluids or cell culture using ultracentrifugation (100,000g). Sucrose density gradients are also used in conjunction with ultracentrifugation to further purify exosomes, where they are found in the 1.15 to 1.19 g/ml fraction.[33] Visual confirmation of exosome size and morphology is usually carried out using transmission electron microscopy (TEM) or cryo-electron microscopy (cryo-EM).[34]

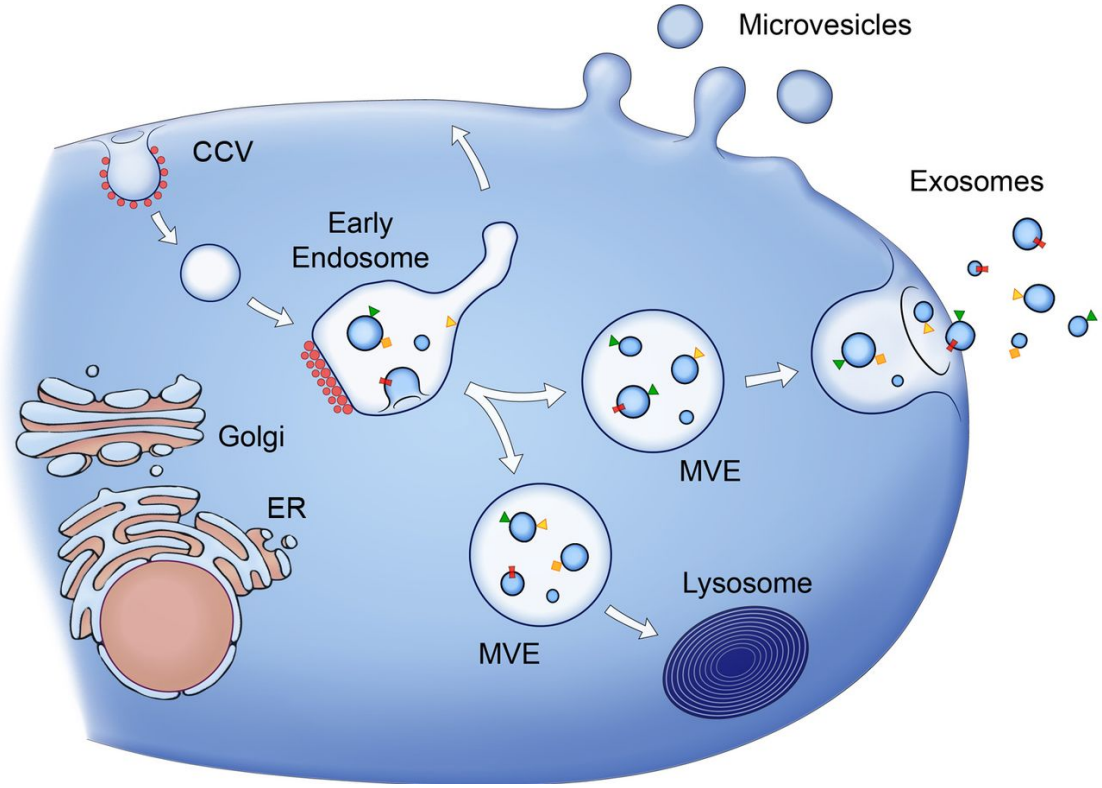


**Figure 1.2.** Cartoon depiction of the formation of exosomes. Adapted from reference 34.

Exosomes carry a cargo that includes proteins, lipids, miRNA and mRNA.[34] Protein characterization in exosomes was initially carried out using immunoblotting, immuno-gold labeling and antibody-coupled to flow cytometry. [35] However, with the development and advent of mass spectrometry based proteomics, over 4000 exosomal proteins have been identified in a variety of exosomes.[36] Exosomes are enriched in plasma membrane,

cytoskeletal, endosomal, and cytosolic proteins. They also carry proteins involved in vesicle transport.[34,35] Tetraspanins, a family of plasma membrane proteins composed of four transmembrane domains, are reported to be highly enriched in exosomes. These include CD63, CD81, CD82, and CD9, which have been used as exosomal markers. It is important to note that no specific marker has been identified for exosomes, and that the protein cargo of exosomes is dependent on the cell source and environmental factors.[37] Exosomes also carry heat shock proteins (Hsc70, Hsc90), cytoskeletal proteins (actin, tubulin, keratin), ESCRT complex proteins (Alix, TSG101) and major histocompatibility complex (MHC) I and II molecules.[36] The protein contents of exosomes shed from MDSC have been reported by Burke et al. and include some expected exosomal proteins such as ESCRT complex proteins and heat shock proteins.[7] Post-translational modifications of proteins in the exosomes have been studied too, to gain a deeper understanding of possible structural and functional role of these proteins in exosomes. I-Hsuan et al. proposed protein phosphorylation in cancer exosomes as breast cancer biomarkers.[38] Ubiquitination of proteins in exosomes has demonstrated possible involvement of the ubiquitin-sensitive ESCRT complex in exosome cargo sorting and biogenesis.[39]

Exosomes are players in facilitating communication in the tumor microenvironment. They can interact with recipient cells in several ways that include direct ligand-receptor interactions, and phagocytosis by the recipient cell. Target cell specificity has been shown to be dependent on integrins carried on the surface of the exosome. Studies conducted by Lyden et al. and Langano et al. have shown that metastatic niche creation is made possible by exosomes and is directed by specific integrins carried by the exosome.[40,41] The case for communication via ligand-receptor interactions is supported by the fact that exosomes carry a host of proteins involved with adhesion on their surface. Buschow et al, have demonstrated that T cells can recruit dendritic cell derived exosomes, which contain MHC class II

molecules.[42] Felicetti et al. have provided visual evidence of exosomes being taken up by recipient cells (Figure 1.3).[43] Investigating the surface proteins of exosomes can lead to a better understanding of the messages exosomes share with recipient cells.

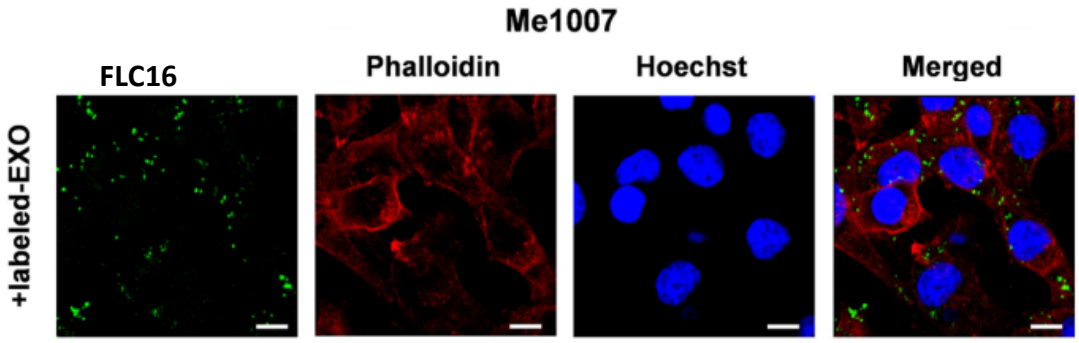


**Figure 1.3.** Visualization of exosomes fused with Me1007 cell line using confocal microscopy. Fluorescent BODIPY® FL C16 was incorporated into lipids of the exosome membranes. Me1007 recipient cells' cytoskeleton was stained with phalloidin (Alexa Fluor 647-red) and nuclei counterstained with Hoechst. (Adapted from reference 40).

MDSC derived exosomes have been the focus of several studies in this laboratory for the last 5 years. Burke et al. first characterized the protein cargoes of exosomes in environments of high (4T1/IL-1) and conventional (4T1) inflammation derived from murine MDSC.[7] The first step in characterizing MDSC derived exosomes was to ensure we had purified MDSC from the mice. After three weeks of inoculation with 4T1 or 4T1 and IL-β, the leukocytes in the blood of the mice is >90% MDSC. Confirmation is carried out using immunofluorescence and flow cytometry of MDSC markers Gr1 and CD11b.[7] The purified MDSC were maintained in serum free medium overnight to collect exosomes and ensure we are only purifying exosomes from MDSC. The exosomes were purified using low speed centrifugation to remove cells, ultracentrifugation to pellet exosomes, and sucrose density fractionation was use to purify the exosomes. Transmission electron microscopy was used to confirm size (50nm diameter) and morphology (circular) of the exosomes. Protein analysis identified the MDSC marker CD11b on the exosomes, as well as pro-inflammatory proteins

S100A8 and S100A9, which are contribute to the immunosuppressive activity of the parental MDSC. Finally, migration assays determined that MDSC derived exosomes are chemotactic for parental MDSC.[7] Therefore, the exosomes purified are also functionally similar to the parental cells. Four hundred and twelve proteins were identified in MDSC-derived exosomes using bottom-up proteomics. Spectral counting showed an increase in abundance for proteins involved in immune responses and membrane budding in animals with heightened inflammation conditions. Exosomes from both conditions carry pro-inflammatory mediators S100A8 and S100A9, which were reported to provide chemotactic activity for MDSC and also to polarize macrophages to a tumor-promoting phenotype.[7] Further studies by Burke et al. also identified ubiquitinated proteins in the cargoes of inflammatory MDSC-derived exosomes. The ubiquitinated protein cohort included several proteins involved in endosomal transport and the pro-inflammatory HMGB1.[44] Top-down proteomics has also been applied to the cargos of MDSC-derived exosomes. Twenty proteins from inflammatory MDSC exosomes and fourteen proteins from conventional MDSC exosomes with several proteoforms have been identified, including 25 proteoforms of S100A8 and 5 proteoforms of S100A9.[20] These and other studies provide further evidence that exosomes do not just carry junk or degraded pieces of proteins out of cells, and that the possible biological functions of exosomes need to be investigated further.

### *1.4. Ubiquitination*

Ubiquitin (Ub) is a protein found in all eukaryotic cells. It is made up of 76 amino acids and acts as a signal by covalently attaching to other proteins. Ubiquitin-like proteins (UbL) are a family of proteins, which include Rub1 and small ubiquitin-related modifier (SUMO).[45] These proteins are similar to Ubiquitin in their amino acid sequences, and this similarity extends itself to the structures of these proteins too. The three dimensional

structures of these proteins are almost superimposable to the structure of Ub, and key residues are maintained between proteins. However, functionally, Ub, Rub1 and SUMO are different. Ub is implicated in protein degradation, sorting, trafficking and regulatory functions. In contrast, the Rub1 protein is involved primarily with regulatory functions and the SUMO proteins regulate cellular processes such as DNA repair and transcription.[46,47] While bacteria do not contain Ub, they have UbL's thiaminS (ThiS) and the molybdopterin synthase surfur carrier subunit protein (MoaD). These prokaryotic proteins have mechanisms of activation similar to Ub and UbL proteins.[45]

Ubiquitin attaches to proteins or to itself as a post-translational modification (PTM) called ubiquitination. Ub can form an isopeptide bond between the carboxyl terminal glycine (G76) and a lysine (K) residue of the substrate protein, or to the initital methionine if the substrate protein is another Ub. A protein could have a single Ub attached (monoubiquitination), or Ub attached at several sites (multiubiquitination). Ubiquitin can form complex internally linked chains since there are eight possible sites of attachment (seven lysines and one methionine) (Figure 1.4). These chains can also be anchored onto other proteins. In addition, polyUb can consist of chains composed of the same linkage site (linear chains) or those with different linkage types (branched chains). It has been ascertained that different linkages of anchored and unanchored Ub chains are responsible for a multitude of linkage specific cellular functions. For example, K48 anchored chains are responsible for proteolytic degradation, K27 anchored chains for host immune response and K6 unanchored chains are involved in mitochondrial quality control.[11]

$M_1$QIFV$K_6$TLTG$K_{11}$TITLEVEPSDTIENV$K_{27}$A$K_{29}$IQD$K_{33}$EGIPPDQQRLIFAG

$K_{48}$QLEDGRTLSDYNIQ$K_{63}$ESTLHLVLRLRGG

**Figure 1.4.** The amino acid sequence of Ubiquitin. The amino acid residues which are potential sites for ubiquitin isopeptide bond formation are highlighted in green. These include the seven lysine residues and the initial methionine.

Several strategies have been developed to identify and characterize ubiquitin chains. Anti-Ub antibodies have been produced to isolate and characterize different forms of ubiquitin. Some of these antibodies have been produced against a specific linkage of ubiquitin, and some are produced for unanchored Ub or polyUb.[48] Immunoprecipitation and/ or western blotting can be used to isolate Ub tagged proteins or unanchored Ub chains from biological samples. However, antibodies are limited in their ability to characterize mixed linkages of Ub chains, and ascertain the number of Ub moieties in the chain. Finally, antibodies have also not been produced for every linkage type possible in ubiquitination, thus some linkages will not be possible to characterize. Another Ub isolation method has been the development of tandem ubiquitin binding entities (TUBES). TUBES are based on ubiquitin associated domains (UBA) found on proteins which bind to Ub.[49] Four of these UBA's are attached in tandem with a linker (Figure 1.5). It has been shown that each of these UBA's can bind to an Ub molecule and also that it does not bind to other UBL's like Nedd8 and SUMO.[50] Commercially available TUBES that bind to polyUb are available. These are not able to distinguish between most of the Ub linkages types, and are available with either equal affinities toward K48 and K63, or just K63. Deubiquitinases (DUBs) are enzymes, which cleave off Ub with linkage specificity. A strategy called UbiCRest (Ubiquitin chain restriction) has been developed which uses DUBs to cleave Ub chains with linkage specificity and thus determine the linkages of ubiquitinated proteins. The UbiCRest method has been implemented effectively to determine the linkages in heterotypic Ub chains.[51,52] However, it

has not been tested on longer Ub chains and is so far limited to analyzing Ub dimers. This analysis is also limited because DUBs specific for every possible Ub linkage type have not been discovered. Finally, mass spectrometry tools have been developed for the detection and evaluation of Ub linkage and topology, which address the limitations in the antibodies, DUBs and TUBES protocols that have been developed.[53,54]

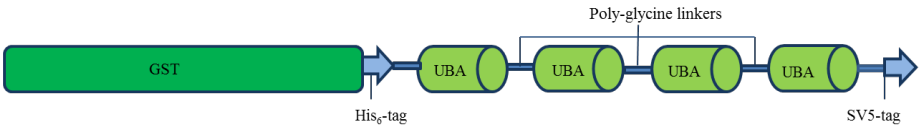


**Figure 1.5.** A cartoon representation of the design of TUBES.

*1.4.1. Bottom up Proteomics*

Enzymes are known for their residue specificity in proteolysis. This feature of the enzymes is exploited as a tool to generate peptides for mass spectrometry analysis. One of the most commonly used and commercially available enzymes is trypsin. Trypsin cleaves peptide bonds at lysine (K) and arginine (R) residues. Tryptic peptides can be introduced into a mass spectrometer after separation by liquid chromatography, to provide a bottom-up proteomics approach. The term bottom-up is refers to a strategy that identifies peptides by mass spectrometry. The peptide precursor and fragment m/z values detected in the mass spectrometer are compared to predicted MS/MS spectral libraries. These spectral libraries are generated by an in silico digestion of protein sequences from a database (the user defines the proteolysis technique used), which results in all possible peptides produced and their predicted MS/MS fragment ion series.[55] Tryptic peptides and bottom-up proteomics have been used by researchers to study the ubiquitiome. Trypsin cleavage leaves a diglycine (-GG) tag on the ε-amine of a lysine residue on the protein targeted by Ub, as it cleaves at R74

(Figure 1.6).[56] The sequencing of peptides by tandem mass spectrometry can identify the addition of mass caused by the site of the addition of the –GG tag on the peptide (114.043 Da). In this way, the location of ubiquitination on the substrate protein can be identified. Linkage sites of unanchored ubiquitin can be determined using tryptic cleavage, as the mass addition of the –GG tag will be located on the linked lysine residue. This method is however, limited in determining the length and topology of the Ub chain attached to the substrate protein, which is crucial in relating to the functional significance of the ubiquitinated protein.

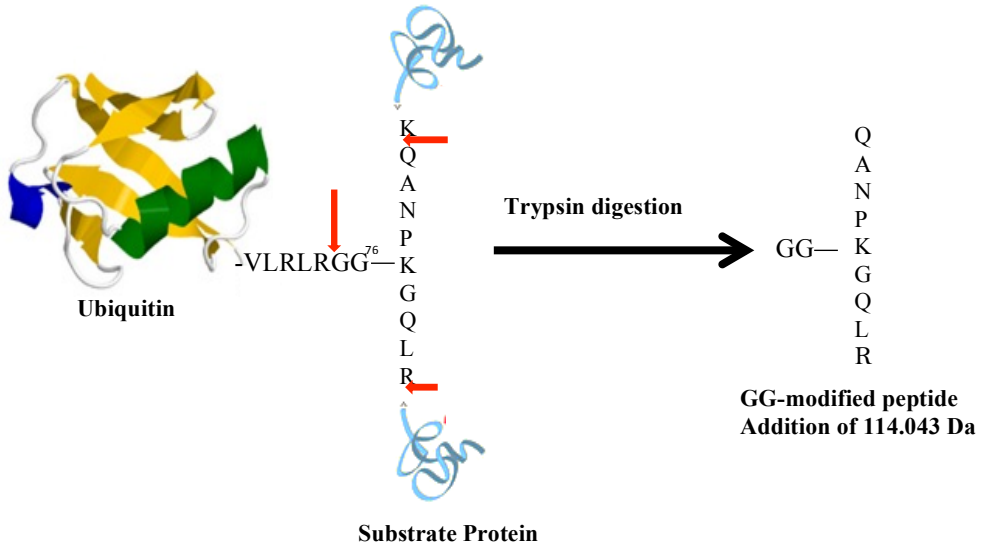


**Figure 1.6**. Cartoon representation of a ubiquitinated protein undergoing cleavage by trypsin. The arginine "R" residue on the Ub gets cleaved and leaves a –GG on the peptide from the substrate protein. The –GG has a mass of 114.043 Da, which is detected by the mass spectrometer.

Bottom-up proteomics has disadvantages when it comes to PTM analysis, as one can only identify a PTM present on one of many peptide. And since protein identifications are

made based on a few peptides, one can lose PTM information. Also, proteins can be found with various forms of PTM's; a bottom-up analysis misses the information of the various possible proteoforms present for each protein identified.

### *1.4.2. Top-down Proteomics*

With the evolution of high-resolution mass spectrometers, an alternative approach to proteomics has been made possible. Top-down proteomics is an approach in which proteins can be analyzed without digestion by an enzyme. In this approach, a protein can be identified and studied with all PTMs present. Top-down analysis allows the user to identify proteoforms and isoforms of the protein/ proteins of interest. Unanchored ubiquitin chains of dimers, trimer and tetramers, including their topological isomers have been distinguished and studied using top-down mass spectrometry.[53,54] The studies take advantage of the high resolution Fusion Lumos instrument, and ETD (electron transfer dissociation) fragmentation in conjunction with supplemental CID (collisional induced dissociation) or HCD (higher-energy collisional dissociation) fragmentation capability available. The study is made possible because the different linkages of Ub produce fragments with unique masses, which are specific for the selected linkage. It is now possible to differentiate polyUb topology and linkage length. The next challenge we face is to isolate endogenous ubiquitinated proteins from a biological sample and apply the methods established to read the ubiquitin code reading strategy.

## *1.5. Protein Analysis by Mass Spectrometry*

### *1.5.1. Orbitrap LTQ-XL Mass Spectrometer*

The orbitrap mass analyzer was first developed in the 1990's. This mass analyzer was developed as a way to optimize the Fourier transform ion cyclotron resonance mass spectrometry device's (FTICR's) ability to discern ions with a small difference in mass-to-charge (m/z) values from biological samples. The advantage of this mass analyzer is that there is no need for a magnetic field because ion trapping occurs with the use of electrostatic fields.[57] The LTQ orbitrap-XL was one of the first commercially available orbitrap instruments provided by ThermoFisher Scientific. This is a hybrid instrument (Figure 1.7), which combines a linear ion trap mass analyzer with an orbitrap mass analyzer, this allowed for high resolution analysis with the speed and sensitivity required for liquid chromatography (LC) time scale analysis of complex mixtures. The resolving power of this instrument is a maximum of 140,000 at 200m/z, which enables studies of small proteins and large peptides.[58] Precursor ions are first accumulated in the C-trap, and then sent to the orbitrap for mass analysis. The C-trap was added to interface the continuously operating electrospray source with the orbitrap, which does not operate in a continuous fashion. Once the ions are in the orbitrap, the mass/charge ratio is measured by recording the frequency of the ions' oscillations inside the trap. Precursor ions are selected for fragmentation either by collision-induced dissociation (CID), electron transfer dissociation (ETD) or higher-energy collision dissociation (HCD). Fragmentation using CID and ETD occur in the linear ion trap and fragmentation by HCD occurs in the multipole region (HCD collision cell) of the mass spectrometer (Figure 1.7). For bottom-up analysis of peptides, the most common method of analysis by the orbitrap LTQ-XL is to acquire a high resolution full MS scan using the orbitrap, and then a data-dependent scan using tandem mass spectrometry (MS/MS) scan in the linear ion trap with CID fragmentation.

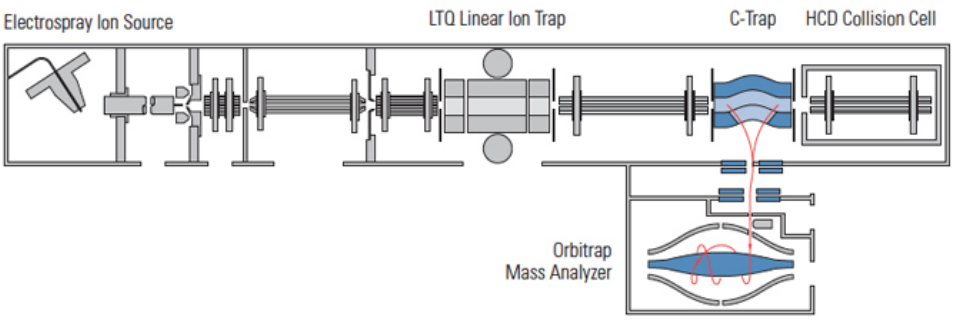


**Figure 1.7.** Overview of the orbitrap LTQ-XL. (http://planetorbitrap.com).

*1.5.2. Orbitrap Fusion Lumos Mass Spectrometer*

The latest innovation in orbitrap mass analyzers is the orbitrap Fusion Lumos tribrid by ThermoFisher Scientific. This instrument has the newer high-field (HF) orbitrap, which provides a higher resolving power (240,000 at 200m/z) without compromising sensitivity. The instrument is able to achieve a lower vacuum with a more efficient pumping system, which allows for more efficient transfer of ions to the orbitrap for mass analysis. Precursor isolation was also improved upon by allowing selection at the quadropole located at the front end of the system (Figure 1.6). Fragmentation using CID and ETD is improved upon when compared to the LTQ-XL by providing a high-pressure cell in the linear ion trap, which increases the efficiency of fragmentation. In the LTQ-XL, the ETD source was at the back of the instrument (Figure 1.5). It has now been moved to the front of the instrument (Figure 1.6). The ETD reagent fluoranthene anion is generated along with cation and neutral products. As it passes through the advanced active beam guide, the anion is separated from the other species, which ensures better ETD fragmentation.

For a bottom-up, discovery based experiment one advantage of using the orbitrap Fusion Lumos is that the full scan in the orbitrap can occur in parallel with the MS/MS scan in the linear ion trap. This allows for the collection of more MS/MS scans, which leads to an

increase in the number of peptides identified. Finally, the instrument provides two different modes for precursor selection for the MS/MS scan. Previously selection of precursor was limited to the Top N mode, in which the user defines the maximum number of precursors that can be targeted per cycle. The orbitrap fusion lumos allows for an extra mode called Top Speed, which allows the user to define a fixed cycle time for MS/MS scans. This allows for the system to perform a maximum number of MS/MS scans in the cycle time defined by the user.

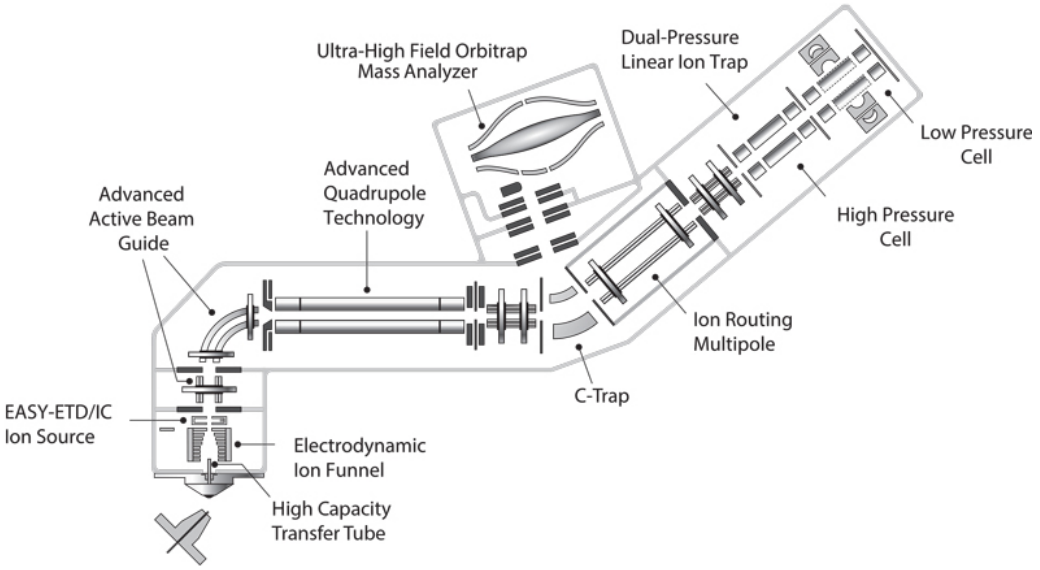


**Figure 1.9.** Overview of the orbitrap Fusion Lumos. (http://planetorbitrap.com).

# Chapter 2: Identification of surface glycoproteins on MDSC derived exosomes and parental cells.

This chapter has been published as a peer reviewed journal article in the Journal of Proteomics Research.

Year-**2017**

Volume-16

Pages- 238–246.

D.O.I- 10.1021/acs.jproteome.6b00811

Title- Surface Glycoproteins of Exosomes Shed by Myeloid-Derived Suppressor Cells Contribute to Function

Authors- Sitara Chauhan, Steven Danielson, Virginia Clements, Nathan Edwards, Suzanne Ostrand-Rosenberg, and Catherine Fenselau

Submitted- September 6, 2016

Publication Date (Web)- October 11, 2016

The following are the contributions of the authors on this list-

Sitara Chauhan- performed the surface glycoprotein enrichments and mass spectrometry analysis.

Dr. Steven Danielson- provided an analysis of one biological replicate of the exosomes surface proteome on the orbitrap fusion lumos mass spectrometer.

Virginia Clements- provided animal husbandry care, performed MDSC and exosomes harvesting, and MDSC migration and chemotaxis assays.

Dr. Nathan Edwards- served as an advisor for the bioinformatics section of this paper.

Dr. Suzanne Ostrand-Rosenberg- directed animal husbandry care, MDSC and exosomes harvesting, and MDSC migration and chemotaxis assays.

Dr. Catherine Fenselau- served as advisor for exosome and cell surface chemistry and mass spectrometry.

*2.1. Introduction*

Proteins on cell surfaces are mediators of cell functions, serving as receptors, transporters, and adhesives. They transport nutrition and waste, respond to stimuli from the environment, and protect the integrity of the cell. They can also serve as ligands for receptors on other cells and deliver signals to surrounding cells in their locale. In the context of the tumor microenvironment, CD47 and other surface proteins are considered drug target candidates,[59,60] as well as biomarkers for distinguishing cells of interest.[61,62] Exosomes, nanoscale vesicles released by almost all types of cells, have been shown to carry cargos that include proteins, lipids, and RNAs and to differ according to the type of parental cells. Exosomes are bounded by a phospholipid bilayer that contains tetraspanins and other proteins. Tetraspanins CD63, CD81, CD82, and CD9 have been proposed as markers of exosomes.[37,63,64] Electron micrographs of immunolabeled CD63 clearly show the protein on the surface of blood-derived exosomes.[65]Several other studies also report visualization of selected proteins on the surfaces of exosomes.[63,66,67] Recent work has highlighted the role that integrins on the surface of exosomes play in uptake by recipient cells leading to premetastatic niche formation and cancer cell migration.[40,41] Here we report an unbiased study of glycoproteins on the surface of exosomes released by myeloid-derived suppressor cells (MDSCs). Our broad objectives are to identify therapeutic targets for reducing MDSC suppressive functions and to gain insight into cell-to-cell communication within the tumor microenvironment that promotes tumor progression

MDSC are immature myeloid cells. They accumulate in the blood and tumor microenvironment of virtually all cancer patients and tumor-bearing mice. They are an acknowledged obstacle to innate anti-tumor immunity and to cancer immunotherapies.[68] MDSC are multifunctional cells that use a variety of suppressive mechanisms to inactivate anti-tumor immunity. They (i) inhibit the activation of tumor-reactive T cells through their

production of reactive oxygen and nitrogen species and by sequestering or degrading amino acids that are essential for T cell function; (ii) polarize immunity and macrophages towards a type 2 phenotype that supports tumor growth; (iii) prevent naïve T cells from entering lymph nodes and becoming activated by down-regulating T cell expression of L-selectin; (iv) inhibit the cytotoxic activity of natural killer cells; (v) promote neo-vascularization through their production of vascular endothelial growth factor (VEGF); and (vi) promote metastasis through their production of matrix metalloproteases.[12]

The inflammatory milieu present in most solid tumors exacerbates both the quantity and potency of MDSC and induces their differentiation and accumulation from hematopoietic progenitor cells.[15,21,69] MDSC mediate most of their immune suppressive and tumor-promoting functions within the tumor microenvironment (TME). Therefore, MDSC function requires that the cells migrate from the bone marrow where they are generated, into solid tumors.[12] Cell-to-cell interactions, such as those between MDSC and their target cells, are frequently initiated by contact between plasma membrane receptors and their soluble or membrane-bound ligands. MDSC and other cells in the tumor microenvironment release exosomes, which also facilitate communication between cells and promote tumor growth and metastasis.[7,70,71] Glycoproteins, such as the Receptor for Advanced Glycation Endproducts (RAGE), facilitate the activation of MDSC.[72] Our previous studies using proteomic approaches demonstrated that exosomes released by MDSC contain one of the ligands for RAGE,[72] and that these proteins are chemotactic for parental MDSC and also polarize macrophages towards a tumor-promoting M2 phenotype.[7] Based on these findings, we hypothesized that proteomic approaches may be useful for identifying additional MDSC plasma membrane and exosomal glycoproteins which may regulate MDSC function and migration.

A number of methods have been developed to take advantage of the unique accessibility of molecules at the surfaces of intact cells. These include lectin affinity columns,[73]alkylation of accessible lysine residues with linked biotin,[74,75] nanoparticle pellicles[76,77] and alkylation of oxidized glycans with linked biotin or hydrazide.[78–81] We have adopted the latter strategy for this study of surface glycoproteins on MDSC-derived exosomes and their parental cells. In particular, the milder oxy-amino alkylation method of Weekes et al[82] was followed because its compatibility with physiological pH minimizes the potential for lysing the exosomes.

We hypothesize that multiple glycoproteins reside on the surface of our exosomes, where they play critical roles in exosome-cell interactions. Here we report the first successful adaptation of cell surface methodology to examine the surface of exosomes released by tumor-induced mouse MDSC. The diameters of these exosomes average around 30 nm, on the small end of the range reported for exosomes.[69] With a high radius of curvature and a small surface area, these vesicles provide an appropriate challenge for surface chemistry. We have characterized 21 glycoproteins, and show that these meet several criteria for a surface origin. We have carried out a parallel identification of ninety-three glycoproteins on the surface of parental MDSC, and discuss similarities in composition that are consistent with the similar functions reported previously for the exosomes and their parent cells. Because MDSC chemotaxis and migration are critical for MDSC function, we have focused our biological studies on CD47, an N-glycosylated integral membrane protein identified by our proteomic studies. We report here that CD47, known for its ability to protect cancer cells from phagocytosis, is also used by MDSC-derived exosomes to chemoattract MDSC.

## *Section 2.2 Experimental Methods*

### *2.2.1. Myeloid-Derived Suppressor Cells and Exosome harvesting.*

Female BALB/c mice, 6-10 weeks of age (bred in the University of Maryland Baltimore County animal facility from breeding pairs obtained from The Jackson Laboratory, Bar Harbor, ME), were injected in the mammary fat pad with $1x10^5$ mammary carcinoma 4T1 cells transfected with the IL-1β gene (4T1/IL-1β) cells. Mice were bled from the submandibular vein when tumors were 9-11mm in diameter. MDSC were harvested from the blood, labeled with fluorescently-coupled antibodies to MDSC markers, and assessed by flow cytometry (Beckman/Coulter Cyan ADP) for purity, as reported earlier.[7,17] Cell populations that were >90% pure $Gr1^+CD11b^+$ cells were used in these studies. Approximately $10^8$ MDSC were obtained from 2-3 mice.

Following isolation from mice, MDSC were either frozen in 15% DMSO and stored at -80°C (for studies with intact MDSC) or maintained in serum-free HL-1 media overnight at 37°C (for collection of exosomes), as previously described.[7] After 16 hrs each supernatant containing exosomes was centrifuged at 805xg and 2090xg to remove residual cells and then ultracentrifuged at 100,000xg to pellet the exosomes. In a previous study the pellet was shown to comprise homogeneous exosomes with diameters 25-30 nm and density of 1.2-1.3 g/ml.[7] Pellets containing the exosomes were resuspended in PBS and absorbances were measured at 260 and 280 nm. Protein concentration was assessed by Bradford Quick Start assay (Biorad, Hercules, CA). Exosomes were never frozen and were used fresh within a week of isolation.

*2.2.2. MDSC and Exosome cell surface chemistry*

Approximately $10^8$ MDSC cells were washed with 50 mM PBS ($CaCl_2$, $MgCl_2$, pH 7.4), and then incubated in 1mM sodium periodate in 50 mM PBS ($CaCl_2$, $MgCl_2$, pH 7.4, 5% FBS) for twenty min at 4°C in the dark to oxidize surface glycans. Oxidized glycans were biotinylated in 100 μM aminooxy-biotin and 10 mM aniline (in PBS with $CaCl_2$, $MgCl_2$, 5% FBS, pH6.7) for 1 hr at 4 °C, washed two times with PBS ($CaCl_2$, $MgCl_2$, pH 7.4) (centrifuged 5 minutes at 900xg), and then re-suspended in lysis buffer (150 mM NaCl, 5 mM IAA, 10 mM Tris-HCl, triton X-100, and protease inhibitor cocktail) and incubated overnight at 4 °C. The following day, mechanical lysis was carried out. The nuclear material and debris was removed by two 40 min centrifugations at 2,800xg, followed by two 40 min centrifugations at 16,000xg. During the final centrifugation streptavidin beads were prepared in snap cap spin columns (Pierce, Rockford, IL) via two washes (one min at 1,000xg) in lysis buffer. The cell lysate was incubated on-column for 2 hr at 4 °C. The beads were washed with lysis buffer and PBS (pH 7.4 0.5 % SDS). Proteins were reduced on column with 100 mM DTT in PBS (pH 7.4 0.5 % SDS) for 20 min at room temperature. The beads were then washed with urea containing (UC) buffer (6 M urea, 100mM Tris-HCl) and alkylated with 50mM iodoacetamide (IAA) in UC buffer for 20 min at room temperature. The biotinylated glycoproteins were digested on-column using 5μg of trypsin in 50 mM ammonium bicarbonate at room temperature, overnight. The tryptic peptides, released from the beads and present in the supernatant were collected by centrifugation, and a C18 column cleanup was performed. The snap cap columns were washed with PBS, followed by milliQ water, and G7 buffer (50 mM sodium phosphate). The N-glycopeptides (still attached to the beads) were released via digestion with PNGase F (15,000 U) overnight in G7 buffer at 37 °C. The

peptides were eluted from the beads and are present in the supernatant, which was then collected by centrifugation.

Preparation of surface proteins from exosomes was performed with starting material of exosomes collected from $1x10^9$ MDSC. The exosomes were incubated in 1 mM sodium periodate in 50 mM PBS ($CaCl_2$, $MgCl_2$, pH 7.4) for twenty minutes at 4 °C in the dark and then centrifuged at 100,000xg for 70 minutes. Exosome pellet was washed with PBS ($CaCl_2$, $MgCl_2$, pH 7.4, 2% BSA), and another 100,000xg spin was performed. The supernatant was removed and the pellet was resuspended in a solution of 100µM amino-oxy-biotin and 10 mM aniline (in PBS, w/$CaCl_2$, $MgCl_2$ 2% BSA, pH 6.7) and incubated for 1 hour at 4°C. Intact exosomes were then washed with PBS ($CaCl_2$, $MgCl_2$, pH 7.4, 2% BSA) (70min, 100,000xg), and then re-suspended in 100 µl PBS (pH 7.4) and incubated overnight at 4°C. The following day exosomes were lysed in 8 M urea. Fifty milimolar $NH_4HCO_3$ was added to each sample to dilute the final urea concentration to 0.8 M. Streptavidin beads were prepared in snap cap spin columns. The exosome lysate was incubated on-column for 2 hr at 4°C. The beads were washed with ammonium bicarbonate and PBS (pH 7.4 0.5% SDS). Proteins were reduced on column with 100mM DTT in PBS (pH 7.4 0.5% SDS) for 20 minutes at room temperature. The beads were then washed with UC buffer and alkylated with 50mM IAA in UC buffer for 20 min at room temperature. The biotinylated glycoproteins were digested on-column using 0.75 µg of trypsin in 50 mM ammonium bicarbonate. The tryptic peptides were collected by centrifugation, and a C18 column cleanup was performed. The snap cap columns were washed twice with PBS, followed by two washes with milliQ water, and two more washes with G7 buffer. The N-glycopeptides (still attached to the beads) were released via digestion with PNGase F (15,000 U) overnight in G7 buffer at 37°C, and collected by centrifugation.

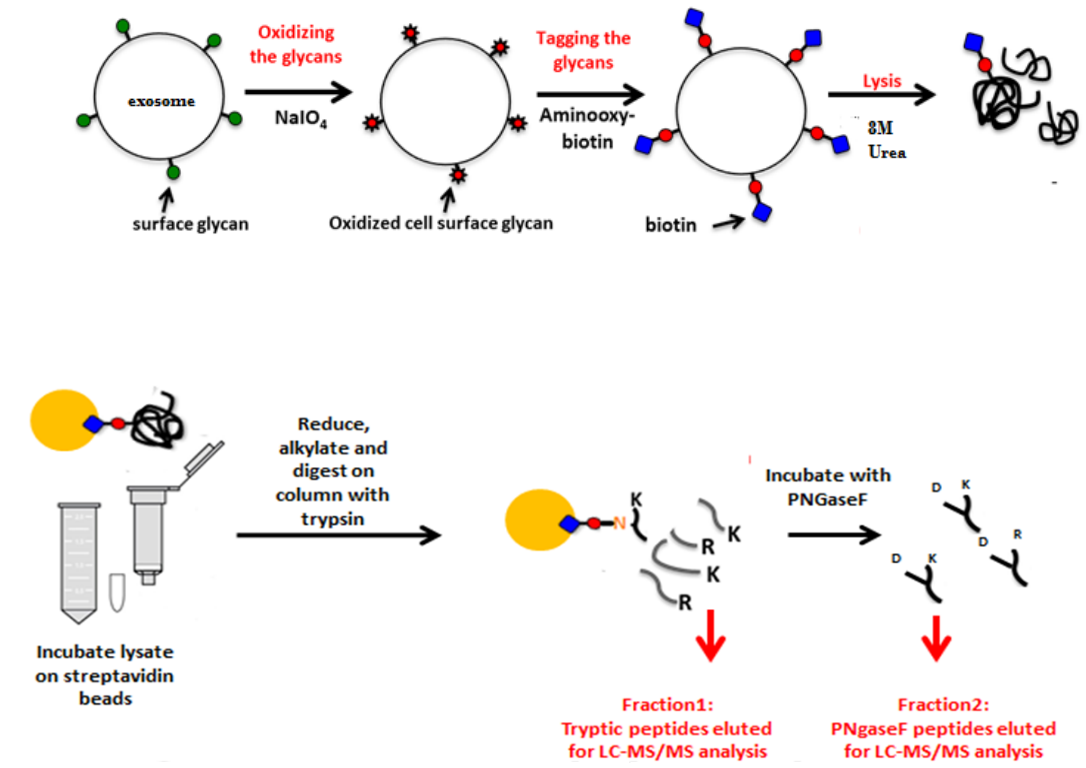


**Figure 2.1.** Cartoon representation of the surface glycoprotein enrichment strategy used.

*2.2.3. HPLC-MS/MS Analysis.*

Tryptic peptides and glycopeptides from both MDSC and exosome samples were fractionated on a C18 analytical column (Grace Vydac, Deerfield, IL) in line with an LTQ-orbitrap XL (Thermo Scientific, San Jose, CA) with a combined linear gradient of 0- 40% solvent B (97.5% CAN (acetonitrile), 2.5% $H_2O$, and 0.1% formic acid) over 140 min and 40 to 85% solvent B over an additional 25 min. The flow rate was 500nL/min. Precursor ion scans were recorded at a resolution of 30,000 at 400 m/z in the orbitrap. In each cycle the nine most highly abundant precursor ions were isolated for fragmentation via collisional induced dissociation (CID) in the ion trap. Fragment ions were analyzed in the ion trap. Samples from one biological replicate each of the parental cells were also analyzed on an orbitrap Fusion. In this case peptides from parental cells were fractionated on a C18 Easy Spray Column 75 µm ID x 25 cm (Thermo Scientific, San Jose, CA) with a linear gradient of

5-32% acetonitrile/ 0.1% formic acid through 120 min at a flow rate of 500 nL/min. Spectra were acquired using a resolution of 120,000 (at 200 m/z) for full scans, followed by HCD fragmentation and detection of the fragment ions in the ion trap in the Top N mode.

In total three biological replicates were analyzed for MDSC and four for the MDSC exosomes. Between three and six injections were examined for each biological replicate.

*2.2.4. Bioinformatics*

Spectra were converted to peak lists and reformatted as mzXML using msconvert from the ProteoWizard project[83] and uploaded to the PepArML peptide identification meta-search engine[84] for searching using MS-GF+.[85] Spectra were searched against the UniProtKB reviewed mouse reference proteome (August 2015). Precursor ion tolerance of 0.05 Da was required for either the monoisotopic or first 13C peak of the precursor isotope cluster, and tolerance of 0.5 Da was used for fragment ion matching. A fixed carbamidomethylation Cys modification was specified throughout. Peptides were required to match the trypsin proteolytic digest motif at both the N- and C- terminus. Up to two missed trypsin cleavages were permitted. Spectral FDR (false discovery rate) was estimated using a reversed protein sequence database.

Peptides in the fraction resulting from PNGaseF deglycosylation and release of glycan-bound tryptic glycopeptides were searched using variable deamidation of Asn residues in the N-X-S/T glycosylation sequence motif and only those peptides with a deamidation mass-shift (+0.98 Da), characteristic of N-glycan cleavage, were retained. Peptides in the fraction resulting from tryptic digestion of bound glycoproteins were searched separately, without this variable modification, and the resulting peptide identifications combined with the PNGaseF fraction deglycosylated glycopeptides. Protein parsimony analysis was applied to the combined exosome and MDSC peptide identifications, after

filtering at 5% spectral FDR, to infer glycoproteins. In addition, at least one deglycosylated glycopeptide identification from the PNGaseF fractions was required for each inferred protein. Proteins inferred on the basis of a single deglycosylated glycopeptide were held to a higher standard, with the single deglycosylated glycopeptide identified required to satisfy spectral FDR at most 1% and to have a unique alignment to UniProt reviewed mouse reference sequences. Protein FDR for the unified parsimony analysis was 2.05%, estimated by tracking decoy peptides and proteins throughout the protein inference procedure.

Nine of the twenty-one exosome proteins were identified based on the identification of a single deglycosylated glycopeptide. Six of these are matched to more than one spectrum. In the parental MDSC cell surface analysis 18 glycoproteins out of 93 were identified based on a single PNGaseF fraction deglycosylated glycopeptide. Stringent one-peptide identifications for the surface proteins have been considered sufficient by other laboratories exploring surface glycoproteins.[86]

The NetNglyc server was used to predict N-Glycosylation sites on peptides identified from the PNGaseF fraction.[87] Uniprot and Protter were used to make predictions on topology domains of the glycopeptides.[88]

*2.2.5. Bioassay for MDSC Chemotaxis*

MDSC chemotaxis with exosomes was assessed as previously described with the following modifications.[7] Intact MDSC from 4T1-tumor-bearing mice (1 x $10^6$ of >90% $Gr1^+CD11b^+$ cells) were placed in the upper chamber of transwells containing an 8μm filter and MDSC-derived exosomes were placed in the lower chamber. In some experiments MDSC-derived exosomes were pre-mixed at 4°C for 1 hr. with 5 μg/ml antibodies to mouse CD47 (clone miap301, Rat IgG2a, catalog #127501, BioLegend), mouse thrombospondin-1 (TSP-1; clone 6.1, catalog #14-9756-82, EBioscience), mouse signal regulatory protein alpha

(SIRPα; CD172a, clone P84, catalog #144002, BioLegend), or the irrelevant isotype matched control antibodies rat IgG2a (clone RTK2758, #400515, BioLegend), mouse IgG1 (clone P.3.6.2.8.15, #16-4714-83, EBioscience), or rat IgG1 (clone BRG1, #16-4301-85, EBioscience), respectively. Pre-incubated exosomes or medium containing no exosomes was then added to the lower chamber of the transwells and the transwells incubated at 37°C, 5% $CO_2$. At the end of 4 hrs, cells migrating to the lower chamber were counted by hemocytometer. In some experiments, parental MDSC were pre-treated at 5μg/ml with the CD47, TSP-1, SIRPα, or corresponding irrelevant isotype matched antibodies for one hour at room temperature, and unbound antibody removed by washing with PBS. Samples were run in triplicate and each sample was counted six times. Values are the average ± SD of triplicate samples per experimental condition. % migration = {experimental-control medium)/ (exosomes-control medium)} x 100%. Statistical analysis was by Student's t- test.

## *2.3. Results and Discussion*

Twenty-one surface N-glycoproteins have been identified on the exosome samples and are listed in Table 2.1. Twenty-one protein identifications were based on twenty-five N-glycopeptide identifications (Appendix 2.1) on twenty-five sites. All glycopeptides contain a motif for N-glycosylation in which an asparagine has been modified (by PNGaseF cleavage) to aspartic acid. Sixteen of the glycosylation sites have been previously identified in other studies using experimental methods,[89] and nine are characterized here for the first

**Table 2.1.** N-Glycoproteins identified on the surface of exosomes released by MSDC. Asparagine residues in the motif N-X-S/T, which were deamidated upon release by PNGase F, are highlighted in red.

| Glycopeptide | Uniprot accession number | Protein |
|---|---|---|
| DQCIVDDITYNV**N**DTFHK | P11276 | Fibronectin |
| LDAPTNLQFV**N**ETDR | P11276 | Fibronectin |
| TEAADLCQAF**N**STLPTMDQ MK | P15379 | CD44 |
| I**N**LTTNVVDVNRPLPLAAY NNR | Q3UZZ4 | Olfactomedin-4 |
| DAMVG**N**YTCEVTELSR | Q61735 | Leukocyte surface antigen CD47 |
| DSSGVINVML**N**GSEPK | Q64277 | ADP-ribosyl cyclase/ CD157 |
| AV**N**QTGALYQCDYSTSR | P05555 | Integrin alpha-M/ CD11b |
| L**N**YTLVGEPLR | P05555 | Integrin alpha-M/ CD11b |
| YL**N**FTASEMTSK | P05555 | Integrin alpha-M/ CD11b |
| ISE**N**GSSVAGILSSPNMEK | Q9Z0M6 | CD97 |
| VVIRPFYLT**N**STDMV | Q07797 | Galectin-3-binding protein |
| VV**N**VSELYGTPCTK | P55772 | Ectonucleoside triphosphate diphosphohydrolase 1/ CD39 |
| DCIQSGPGCSWCQKL**N**FTG PGEPDSLR | P11835 | Integrin beta-2/ CD18 |
| AFM**N**SSFTIDPK | O88792 | Junctional adhesion molecule A/ CD321 |
| ALMPFDSLHDDPCLLT**N**R( S) | P11247 | Myeloperoxidase |
| KVSCPIMPCS**N**ATVPDGEC CPR | P35441 | Thrombospondin-1 |
| VV**N**STTGPGEHLR | P35441 | Thrombospondin-1 |
| GFCEAD**N**STVSENNPEDWP VNTEGCMEK | P40237 | CD82 |
| FLEQQNQVLQTKWELLQQ V**N**TSTR | Q6IFZ6 | Keratin, type II cytoskeletal 1b |
| YKGTAGNALMDGASQLVG E**N**R(T) | Q8K0E8 | Fibrinogen beta chain |
| GTAGNALMDGASQLVGE**N** R(T) | Q8K0E8 | Fibrinogen beta chain |
| VQGCMSQPGCNLL**N**GTQTI GPVDVSER | Q8R2S8 | CD177 |
| AELS**N**VSDTVWNIR | Q9D8U6 | Mast cell-expressed membrane protein 1 |
| IVDV**N**LTSEGK | Q9ET30 | Transmembrane 9 superfamily member 3 |
| AL**N**ASQEETGAVFLCPWK | Q9QUM0 | Integrin alpha-IIb/ CD41 |
| LLENCGF**N**MTAK | Q9WVG5 | Endothelial lipase |

From the surface of the parental MDSC, 188 N-linked glycopeptides were characterized, supporting the identification of 93 glycoproteins (Appendix 2.2). On sixteen of these glycopeptides we identified glycosylation at two sites. In all, 204 glycosites are identified. One hundred and fifty-two of the 204 observed sites of N-glycosylation have already been confirmed by experimental evidence in other studies[89] while 52 are characterized for the first time here. Twenty-seven of the latter cohorts are not predicted by the NetNGlyc database (Appendix 2.3).

The topological domains of the N-linked glycosites identified from the exosomal surface were also evaluated, seeking confirmation of the fidelity of oxidative alkylation on the surface of our exosomes (Appendix 2.4). Based on the chemistry, we would expect all the glycopeptides observed to originate in solvent accessible regions of the proteins. Relevant topologic information is not available for all of the proteins, however the majority of glycosites identified on the surface of the exosomes, and also on the parental MDSC surface, can be assigned to extracellular regions of their proteins. A few glycosites originate from proteins in the extracellular space and some from GPI anchored proteins that do not have transmembrane domains (Fig.2.2).

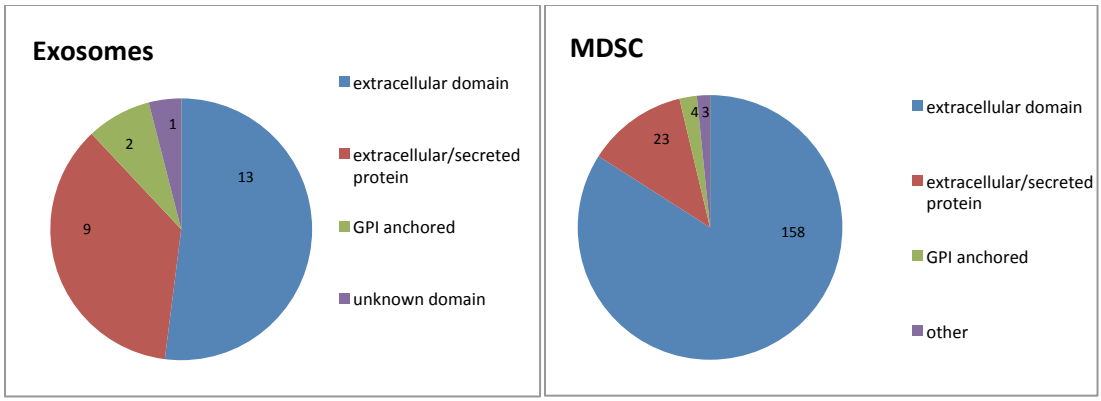


**Figure 2.2.** Origins of N-linked glycopeptides identified on the surfaces of parental MDSC and exosomal N-glycopeptides. The topology information was created using Uniprot and Protter.

Cluster of differentiation (CD) proteins (named after a protocol used for the identification of cell surface molecules) are of particular interest because of their interactive functions at the cell surface. Ten CD proteins were identified on the exosomes, and thirty-five on MDSC (Fig. 2.3). The CD proteins found on surfaces of both parental cells and exosomes include CD11b (also known as Mac-1), which is used as a marker for MDSC although it is also expressed on other hematopoietic cells. CD47 was also found on both surfaces and is of interest as it is reported to prevent phagocytosis by macrophages and thereby protects cancer cells from immune destruction.[90] CD82 found on both surfaces is known to bind to CD4 and stimulate the T-cell receptor signaling cascade.[91]

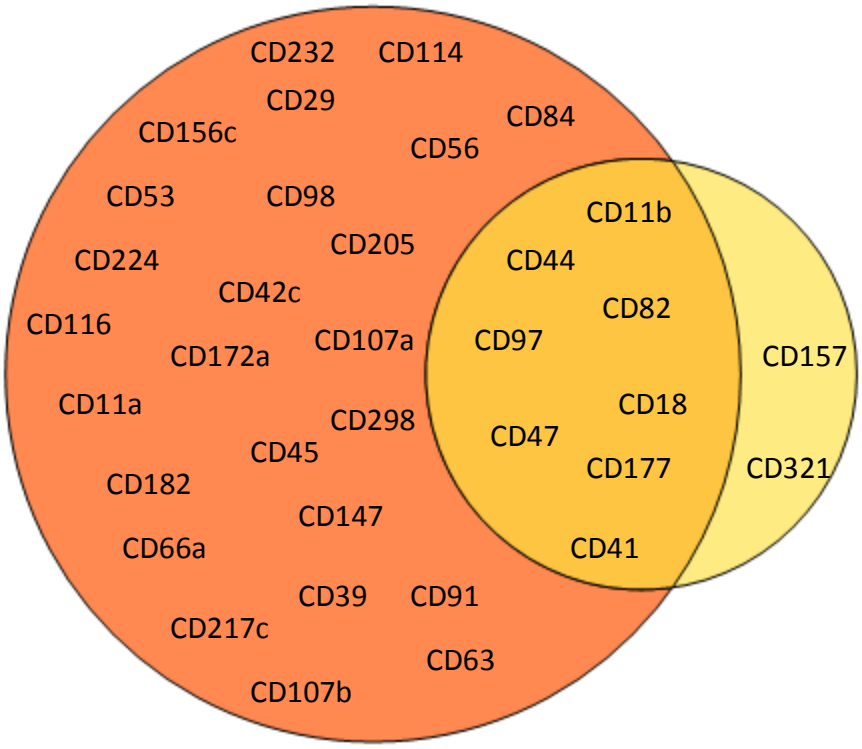


**Figure 2.3.** CD proteins identified on the surfaces of the MDSC and MDSC derived exosomes.

The similarity or difference between proteins carried by exosomes and their parental cells is of considerable interest to researchers studying the role of exosomes in intercellular communication.[92–94] In the present study, 17 of the 21 exosome glycoproteins were found in common on the surface of parental MDSC with N-linked glycopeptide identifications on exosomes. Another three proteins identified on the basis of N-glycopeptides in exosomes are supported by tryptic peptides in MDSC (ADP-ribosyl cyclase (CD157), transmembrane 9 superfamily member 3, and endothelial lipase) (Appendix 2.5). Only junctional adhesion molecule A (CD321) was identified on the exosome surface but not detected at all in our current examination of parental MDSC samples. Intriguingly, ADP-ribosyl cyclase (CD157) is identified in the exosomes by virtue of one deglycosylated glycopeptide and no tryptic peptides, while in the parental MDSC, four distinct tryptic peptides were observed, but no

deglycosylated glycopeptide, suggesting it is differentially glycosylated in exosomes. The overlap between exosome and parental MDSC surface proteins demonstrated here exceeds 80% (17 of 21 proteins) and suggests that the surface of the exosomes primarily carry proteins representative of the surface of the primary cells that released them.

Exosomes are proposed to transport active biomolecules from sender cells to receiver cells, a hypothesis that raises questions about recognition and adhesion (as well as transmembrane mechanisms).[95–99] We have shown that MDSC exosomes stimulate migration of MDSC,[7] and we have summarized in Table 2.2 glycoproteins known to be partners in receptor/ligand interactions and thus, potentially, in MDSC/exosome couplings. Leukocyte surface antigen (CD47) and CD44 on the exosome surface both bind glycoproteins identified on the MDSC surface[100,101] and CD29 and CD172a on the MDSC surface bind to TSP-1,[102] and fibrinogen,[103] respectively, identified on the exosome surface. Most of the cell surface molecules listed in Table 2.2. are also receptors or ligands expressed by other cells in the tumor microenvironment.[104–108] Our survey appears to support adhesion between exosomes and cells, though not yet selective recognition.

**Table 2.2.** Ligand/substrate binding partners identified on the surface of MDSC and MDSC-derived exosomes.

| **Exosome** | **MDSC** |
|---|---|
| integrin alpha-IIb/ CD41 | thrombospondin, fibronectin, fibrinogen |
| integrin alpha-M/ CD11b | haptoglobin, fibrinogen, fibronectin |
| integrin beta-2/ CD18 | haptoglobin, fibrinogen |
| leukocyte surface antigen (CD47) | thrombospondin-1, CD172a |
| CD44 | Fibronectin |
| thrombospondin-1 | CD29, leukocyte surface antigen (CD47) |

MDSC-derived exosomes exhibit immunosuppressive functionalities similar to that of their parental cells[7] and proteins on their surface should similarly be considered as potential drug targets. Neutrophil granule protein is a protein of interest identified in this

study on the surfaces of both MDSC and MDSC-derived exosomes. CD47 is particularly interesting because cancer cells express elevated levels of CD47, which sends a "don't eat me" signal when it complexes with CD172a (signal regulatory protein alpha or SIRPα), thereby preventing phagocytosis by macrophages.[90] CD47 is also known to affect cellular aggregation and migration, [109] and it is currently under investigation as a potential therapeutic target against cancer.[59,60] These characteristics made CD47 an interesting candidate for functional assays.

MDSC mediate their immune suppressive functions within the tumor microenvironment. Since MDSC are generated in the bone marrow and traffic via the circulatory system, their entry into solid tumors involves chemo attraction. Our previous studies have demonstrated that tumor-derived inflammatory factors[72] and MDSC-derived exosomes facilitate this chemoattraction.[7] The ability of the MDSC to sense a chemoattraction signal is studied using transwell migration assays. Transwell migration assays consist of cells being placed on the upper chamber of a transwell with a semi-permeable membrane. The lower chamber has a solution that contains cells or exosomes, which generate the chemoattractant signal. The cells in the upper chamber cannot fall through the semi-permeable membrane, but need to change shape in a process that mimics extravasation in order to cross over to the lower chamber. This migration of the cells from the upper to the lower chamber is a result of the chemoattractant signal released by cells or exosomes in the lower chamber.[110] In the case of our studies, we expect that secreted proteins from cells in the upper chamber will be released, and move to the lower chamber through the semipermeable membrane. The secreted proteins will bind to their receptor on the surface of either cells or exosomes in the bottom chamber, which will lead to the release of chemotactic molecules. The released cytokines serve as a chemoattractant to the cells in the upper chamber, which will then migrate to the lower chamber and be counted at the end of the

duration of the assay. We first confirmed by flow cytometry that parental MDSC express cell surface CD47 by staining MDSC with an antibody specific to CD47 or an irrelevant isotype matched antibody (Fig. 2.4.A). As expected from the proteomic analysis, MDSC expressed high levels of CD47. To determine if CD47 impacts MDSC migration, we used a transwell system in which MDSC were placed in the upper chamber of a transwell containing a semipermeable membrane, and MDSC-derived exosomes were placed in the lower chamber. Ability of the exosomes to chemoattract parental MDSC was determined by quantifying the number of MDSC migrating into the lower chamber. The role of CD47 was determined by assessing MDSC migration in the presence of an antibody that sterically blocked CD47. In the absence of exosomes, MDSC did not migrate, confirming that exosomes are chemotactic for MDSC. Preincubation of the exosomes with increasing quantities of anti-CD47 antibody, but not an irrelevant control antibody, significantly decreased the number of migrating MDSC (Fig. 2.4B). These results indicate that CD47 facilitates exosome-mediated migration of MDSC.

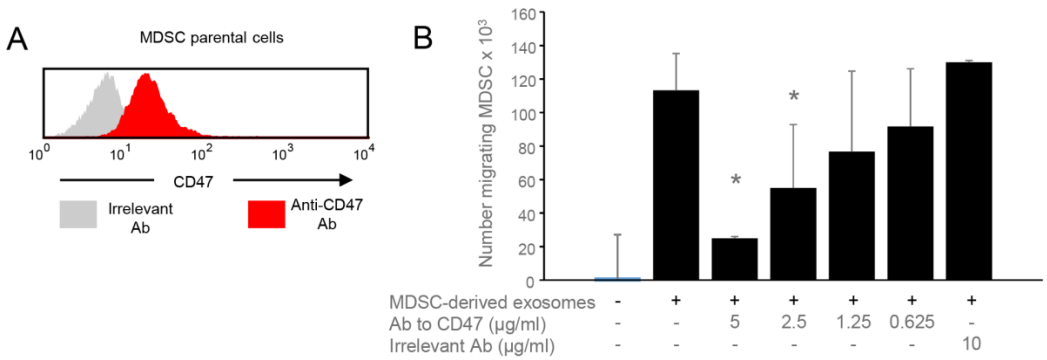


**Figure 2.4.** CD47 regulates MDSC chemotaxis and migration in response to MDSC-derived exosomes. (A) Parental MDSC express CD47 on their cell surface. Tumor-induced MDSC were stained with fluorescent antibody to CD47 or with irrelevant control isotype-matched antibody and analyzed by flow cytometry. (B) BALB/c tumor-induced MDSC were placed in the upper chamber of a transwell and MDSC-derived exosomes, with or without titered quantities of antibody to CD47 or irrelevant control antibody IgG2b were placed in the lower chamber. MDSC migrating to the lower chamber were quantified by counting. * indicates values are statistically significantly different from exosomes without antibody to CD47 or

exosomes with isotype control antibody ($p<0.02$). Data are from one of six independent experiments with 5µg/ml CD47 antibody.

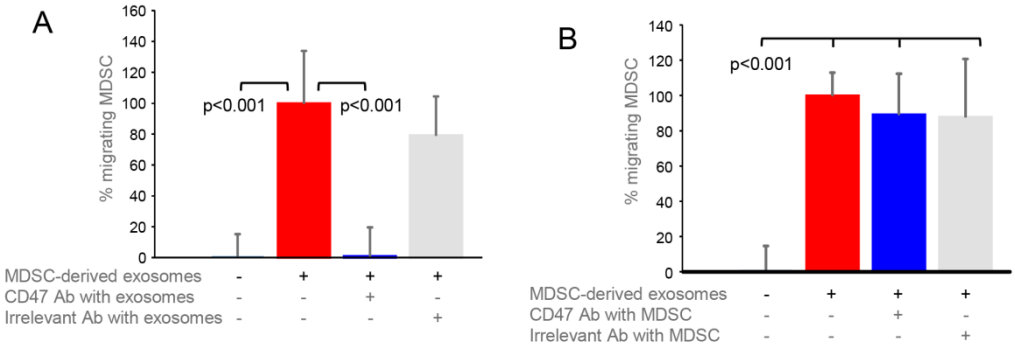


**Figure. 2.5.** CD47 on MDSC-derived exosomes, and not CD47 on intact (parental) MDSC regulates MDSC chemotaxis and migration. Chemotaxis assay was performed as in fig. 1 except (A) exosomes or (B) MDSC in some samples were pre-treated with antibody to CD47 or an irrelevant isotype matched antibody prior to their placement in the transwells. Data are representative of one of six and three independent experiments for (A) and (B), respectively.

CD47 binds two ligands: the secreted protein thrombospondin-1 (TSP-1) and the integral membrane protein SIRPα. Our proteomic analysis identified TSP-1 in both parental MDSC and MDSC-derived exosomes, while SIRPα was only detected in the parental MDSC. Exosome driven chemotaxis of MDSC could involve either or both of these ligands and either the MDSC or the exosomes could express the receptor CD47 or the ligand TSP-1 or SIRPα. To determine whether CD47 is used by the MDSC and/or the exosomes, exosomes or MDSC were pre-treated with blocking antibodies to CD47 or an irrelevant control isotype matched antibody prior to inclusion in the migration assay. Anti-CD47 antibody pre-treatment of the exosomes (Fig 2.5A), but not the MDSC (Fig. 2.5B) prevented migration, while the irrelevant antibody had no effect. These results indicate that the exosomes, and not the MDSC use the integral membrane protein CD47 as the receptor. Since the receptor CD47 is functional on the exosomes, MDSC chemotaxis could involve MDSC-produced TSP-1 and/or SIRPα. To determine if either of these ligands are involved, and to ascertain if MDSC are the source of the ligand, exosomes or MDSC were pre-treated with blocking antibodies to TSP-1 or SIRPα

prior to inclusion in the migration assay. Pre-treatment of either exosomes or MDSC with antibodies to TSP-1 significantly decreased MDSC migration (Fig. 2.6A and 2.6B, respectively). Since antibodies cannot be removed from the exosome solution prior to the assay, these anti-TSP-1 antibodies could be neutralizing TSP-1 produced by either the MDSC or exosomes. In contrast, pre-treatment of either exosomes or MDSC with blocking antibodies to SIRPα only minimally reduced MDSC migration and this trend was not statistically significantly different from the effect of the irrelevant antibody controls (Fig. 2.7A and 2.7B, respectively). These results demonstrate that TSP-1 is the dominant CD47 ligand that regulates exosome-driven MDSC chemotaxis.

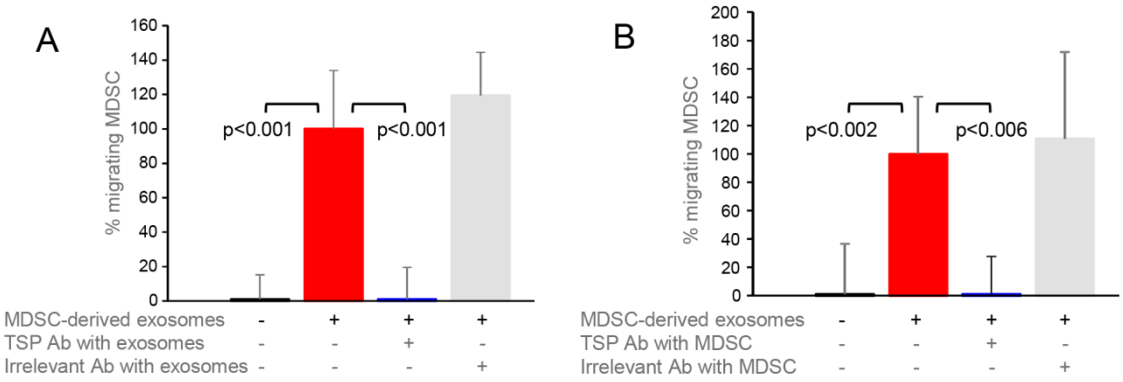


**Figure 2.6.** Thrombospondin-1, a ligand for CD47, is produced by parental MDSC and facilitates MDSC chemotaxis and migration. Chemotaxis assay was performed as in Fig. 1 except (A) exosomes or (B) MDSC in some samples were pre-treated with antibody to thrombospondin (TSP-1) or an irrelevant isotype matched antibody prior to their placement in the transwells. Data are representative of one of three and one of two independent experiments for (A) and (B), respectively.

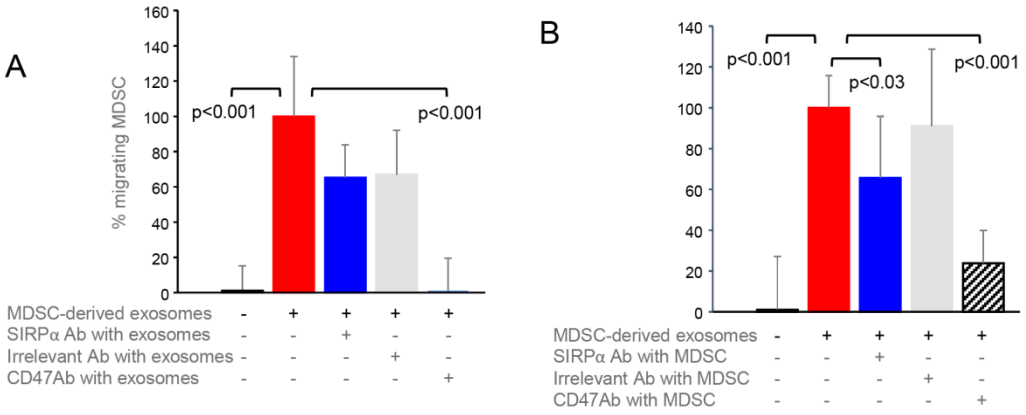


**Figure 2.7.** SIRPα, a ligand for CD47, is produced by parental MDSC and may contribute to MDSC chemotaxis and migration. (A) Chemotaxis assay was performed as in fig. 1 except (A) exosomes or (B) MDSC in some samples were pre-treated with antibody to SIRPα, antibody to CD47, or an irrelevant isotype matched antibody prior to their placement in the transwells. Data are representative of one of three and three independent experiments for (A) and (B), respectively.

## *2.4. Conclusions*

We have successfully established a method to identify glycoproteins on the surfaces of exosomes, and demonstrated that multiple glycoproteins are present on the surface of MDSC-derived exosomes. About 80% of the surface glycoproteins on these exosomes were also identified on the surface of parental MDSC, providing further support to the conclusion that the protein cargo in exosomes closely resembles that of the parent cells. Our studies identified numerous molecules that have the potential to regulate exosome activity and function. For example, exosomes were observed to contain CD321 (also known as junctional adhesion molecule A, encoded by the F11R gene). In addition to its function in cellular tight junctions, CD321 binds to leukocyte function antigen 1 (LFA-1 or CD11a) which we detected in MDSC. LFA-1 is also expressed by T cells raising the possibility that MDSC-

derived exosomes might deliver their immune suppressive cargo to T cells by their binding of CD321 to T cell LFA-1.

The leukocyte surface antigen CD47 and its ligand TSP-1 were among eight CDs found on both cell and exosome surfaces. CD47 is well known for its ability to protect tumor cells from phagocytosis. Our studies demonstrate that CD47 also promotes tumor progression by enhancing the trafficking of immune suppressive MDSC and thereby inhibiting anti-tumor immunity. Therefore, in-progress clinical trials testing the therapeutic effect of antibodies to CD47 may not only demonstrate direct effects on tumor cells, but may also facilitate the development of anti-tumor immunity.[111]

# Chapter 3: Ubiquitome of MDSC derived exosomes under heightened and basal inflammatory conditions.

*This work was jointly authored by Katherine Adams, who performed the sample preparation, and the LC-MS/MS analysis, and Sitara Chauhan, who performed the data processing and analysis. The data collected by Katherine Adams has been published in her master's thesis,*[112]*but has been reanalyzed in this document.*

## *Section 3.1 Introduction*

Myeloid derived suppressor cells accumulate in the tumor microenvironment of experimental mice and patients, where they are able to suppress innate and adaptive immune responses and thus contribute to tumor growth. [13] The accumulation of MDSC in the tumor environment is exacerbated by the presence of proinflammatory mediators.[7,113] These include inflammation-associated molecules vascular endothelial growth factor (VEGF), granulocyte-macrophage colony-stimulation factor (GM-CSF), prostaglandin E2 (PGE2), interleukin 1-beta (IL-1β), and calcium-binding proteins S100A8 and A9 (S100A8/A9). Some of these molecules are shed by tumor cells (prostaglandin E2), and are found to induce differentiation of myeloid cells to form MDSC. IL-1β is another proinflammatory cytokine, which has shown to promote tumor growth through the induction of MDSC.[72]

Increased levels of MDSC are observed when mice are inoculated with tumor cells secreting IL-1β.[7] S100A8 and S100A9 are proinflammatory proteins, which have elevated levels in diseases associated with increased inflammation. Similar to previously discussed cytokines, they lead to accumulation of MDSC, and are also secreted by the MDSC.[72]

Therefore, increases in inflammation, increase the potency of MDSC immune suppressive activity by a host of different factors found in the tumor microenvironment.

The role of inflammation on exosomes shed by the MDSC is therefore worth investigating. A previous study has compared the protein cargoes of exosomes shed by MDSC from a higher inflammatory environment (INF) to exosomes shed by MDSC from a conventional inflammatory environment (CON). This study found that proteins S100A8 and S100A9 were found in both INF and CON exosomes but their relative abundances did not change in exosomes from higher inflammation. The study found 30 proteins to have increased relative abundances in heighted inflammation. Functions of these proteins involved membrane budding, GTP/ATP binding and protein sorting.[7]

Ubiquitination as a post-translational modification (PTM) is involved in the regulation of a multitude of cellular pathways. Many of its functions are based in linkage type, for example K-48 linked Ub chains are involved with tagging proteins for degradation. K-63 linked Ub on the other hand is functionally responsible for the regulation of inflammatory pathways.[114] K-63 linked chains bind to, and activate proteins called pattern recognition receptors, which in turn lead to the activation of NF-κB pathway.[115] The NF-κB pathways has been associated in MDSC function as IL-Iβ has been shown to activate MDSC through the NF-κB pathway.[21]

Extracellular Ub has specifically been shown to affect the functioning of immune responses. Ubiquitin has been discovered in extracellular fluid and has been found to be responsible for differentiation of hematopoietic and lymphocyte cells. A mutation in components of the linear ubiquitin chain assembly complex (LUBAC), which is involved in innate immunity response in mice ad humans, causes immune disorders and activation of the NF-κB pathway. The conjugation of Ub to target proteins can affect antigen processing by

antigen presenting cells, and thus deregulate normal immune responses. Conjugation of Ub to target proteins is carried out by E3 ligases and three specific E3 ligases (casitas B-lineage lymphoma proto-oncogene B [Cbl-b], itchy E3 ubiquitin protein ligase [Itch], and gene related to anergy in lymphocytes [GRAIL]) are known to have increased expression, which then affects T-cell receptor signaling.[116]

In exosomes, ubiquitination has been proposed to influence the sorting of proteins in several ways. Ubiquitination is involved in the internalization of surface proteins,[114] and sorting proteins into luminal vesicles,[117] which eventually give rise to exosomes. The endosomal sorting complexes required for transport (ESCRT) machinery is known to mediate the formation of endosomes and is also thought to participate in the invagination of the limiting membrane to form ILV's, which are later released from the cell as exosomes. The ESCRT proteins- ESCRT-0, –I and, -II contain ubiquitin binding domains, which help them to bind to Ub, and deliver the Ub proteins into the endosomes.[118] Investigators have previously proposed that Ub is removed from proteins that are sequestered into ILVs destined to be released as exosomes.[117,119] However, recent identifications of significant numbers of ubiquitinated proteins in the lysates of exosomes from a variety of cell types are cited to contradict this mechanism.[39] This phenomenon could be explained by the fact that ESCRT-independent sorting mechanisms have been recently identified in the formation of exosomes (Figure 3.1).[34,120] A few studies have discovered that exosomes have an enhanced Ub conjugation to cellular protiens.[39,121] Srinikanth and colleagues found that Ubiquitin in exosomes was responsible for causing degradation of CD63 in macrophages, which results in suppressing platelet thrombosis. These results point to the fact that studying the role of ubiquitination in exosomes and immune responses is of utmost importance and is still not well understood.

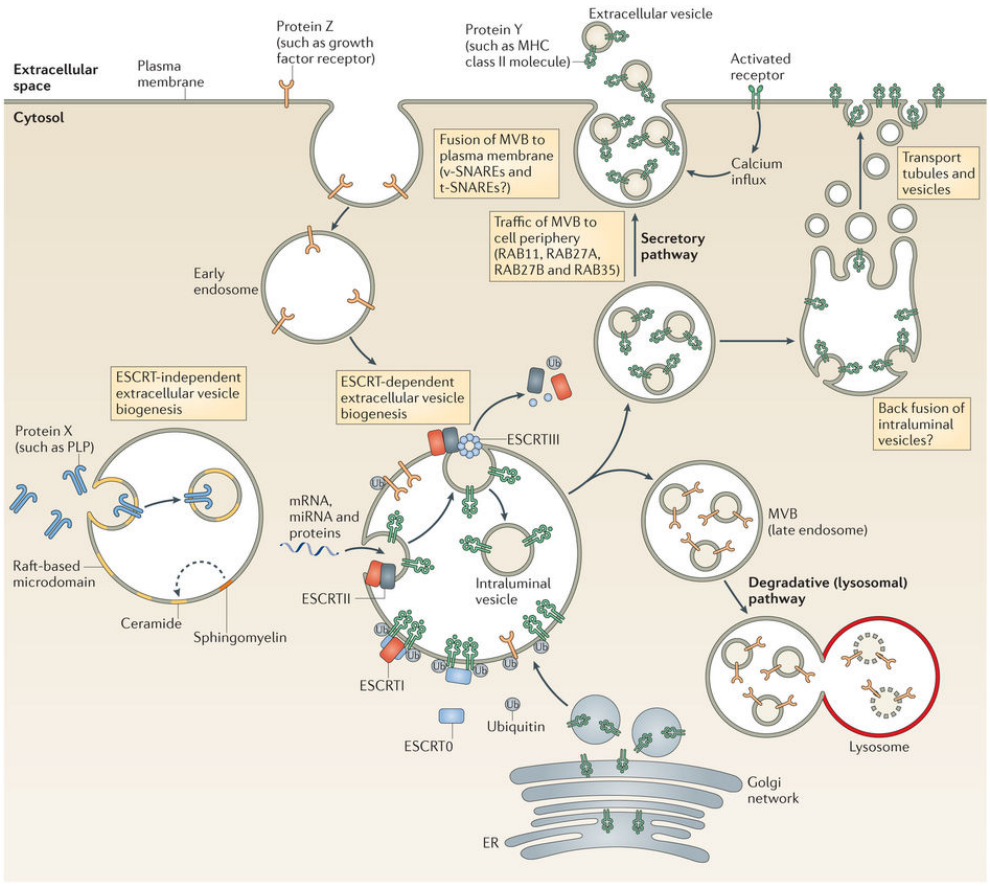


**Figure 3.1.** ESCRT independent and ESCRT dependent pathways regulate the formation of exosomes. Adapted from reference 119.

Polyubiquitination is a large modification; the ubiquitinated proteins are usually present at sub-stoichiometric levels compared to their unmodified proteoforms.[122–124] This can make studying this PTM particularly challenging. However, based on previous studies on exosomal ubiquitinated proteins, we hypothesized that the MDSC-derived exosomes will contain enhanced ubiquitination of their protein cargo. The present study uses state-of-the-art mass spectrometry optimized for bottom-up proteomic analysis to compare the proteomes recovered from exosomes shed by MDSC isolated from tumor-bearing mice with high and low inflammation and to characterize their respective ubiquitomes.

*Section 3.2 Experimental Methods*

*3.2.1. Myeloid-Derived Suppressor Cells and Exosome Harvesting.*

Female BALB/c mice, 6-10 weeks of age (bred in the University of Maryland Baltimore Campus [UMBC] animal facility from breeding pairs obtained from The Jackson Laboratory, Bar Harbor, ME), were injected in the mammary fat pad with 7,000 4T1 cells transfected with the IL-1β gene (4T1/IL-1β) cells. Other mice were injected with 4T1 cells, which were not transfected with IL-1β. Mice were bled from the submandibular vein when tumors were greater than 8 mm in diameter. MDSC were harvested from the blood, labeled with fluorescently-coupled antibodies to MDSC markers, and assessed by flow cytometry (Beckman/Coulter Cyan ADP) for purity.[7,17] Cell populations that were >90% pure $Gr1^{+}CD11b^{+}$ cells were used in these studies. Approximately $10^{8}$ MDSC were obtained from 2-3 mice.

Three biological replicates of exosomes, from each high and low level of inflammation were used for this study. Each replicate of exosomes was collected from 1 x $10^{8}$ MDSC pooled from 2-3 mice. Following isolation from mice, MDSC were maintained in serum-free HL-1 media overnight at 37°C to collect exosomes.[7] After 18 hours, each supernatant containing exosomes was centrifuged at 805xg and 2090xg to remove residual cells and then ultracentrifuged at 100,000xg to pellet the exosomes. Pellets containing the exosomes were resuspended in phosphate buffered saline (PBS) and they were stored at -80°C with deubiquitinase (DUB) inhibitors added.

*3.2.2. Protein Analysis*

Exosomes were lysed by suspension in 8 M urea in 50 mM ammonium bicarbonate with 50 μM deubiquitinase inhibitor PR-619 (LifeSensors, Malvern, PA) and 1% by volume

protease inhibitor cocktail (Sigma-Aldrich, St. Louis, MO). The solution was centrifuged at 13,000 xg for 30 min through a 3 kDa molecular weight cut off filter (Millipore, Darmstadt, Germany), and the filtrate was discarded. This process was performed three times before the buffer was diluted to 0.8 M urea in 50 mM ammonium bicarbonate. Protein content was measured using the Pierce BCA Assay Kit (Thermo Fisher Scientific, San Jose, CA).

A solution containing 25 µg of protein lysate was digested with trypsin. This normalized the amount of total protein between the two samples- CON and INF exosomes. Samples were reduced with 20 mM dithiothreitol (Sigma Aldrich, St. Louis, MO) for 30 min at 56°C and alkylated with 10 mM methyl methanethiosulfonate (Sigma Aldrich, St. Louis, MI) for 45 min. Trypsin (Promega, Madison, WI) was added for a final 1:50 enzyme: protein concentration and digestion was performed overnight at 37°C before addition of 0.1% formic acid. Three technical replicates of 1 µg total protein were prepared and analyzed by LC-MS/MS for each of three biological replicates.

*3.2.3. LC-MS/MS and Bioinformatics Analyses*

A bottom up strategy was used to provide the most inclusive and extensive inventory of MDSC exosomes. LC-MS/MS analyses were performed on an Ultimate 3000 nano-HPLC system (Dionex, Sunnyvale, CA) in-line with an orbitrap Fusion Lumos Tribrid mass spectrometer (Thermo Fisher Scientific, San Jose, CA). A 2 µL aliquot of tryptic peptides was injected onto a C18 column (Dionex, Sunnyvale, CA) and desalted with 10% solvent A (97.5% $H_20$, 2.5% ACN, and 0.1% formic acid) for 10 min. Peptides were fractionated on a C18 column (Dionex, Sunnyvale, CA) with a 2 hr linear gradient at a flow rate of 300 nL/min increasing from 5 to 55% solvent B (97.5% ACN, 2.5% $H_2O$, and 0.1% formic acid) in 90 min, followed by an increase from 55 to 90% solvent B in 5 min, and held at 90% solvent B for 5 min. Precursor scans were acquired in the orbitrap with a resolution of 120,000 at m/z

200. The most abundant ions, as many as possible (Top-Speed mode on Fusion Lumos), during each 3-second duty cycle were selected for fragmentation by collisional induced dissociation (35% collision energy) in the ion trap, and product ion scans were acquired in the ion trap. A dynamic exclusion of one repeat count over 30 seconds was used.

Peptide and protein identifications were carried out using PepArML (28) meta-search engine against the UniProt mouse database (11 2016). Peptide matches were filtered at 1% spectral false discovery rate (FDR), and global protein parsimony required at least 2 unshared peptides. This resulted in a protein FDR of < 3.3%. Fixed modifications listed methylthio modification of cysteine, and variable modifications included oxidation of methionine, glycinylglycine modification of lysine and N-terminal residue pyrrole modifications.

Once the exosomal proteins were identified, additional GG-tagged peptides with at most 10 % spectral FDR were re-introduced to the set of identified peptide spectral matches. The final FDR for the GG-tagged peptides retained using this method was < 5.7%. Proteins with at least one peptide with a lysine residue modified with glycinylglycine (GG-tag) were considered to be ubiquitinated.

Subcellular location and function assignments (relative to the parent cells) were made using the Protein Information Resource GO Slim (http://pir.georgetown.edu) using UniProt Gene Ontology annotations (12 2016). Pathway analysis was carried out using the canonical pathways from the REACTOME database.[125] A pathway enrichment analysis of differentially abundant MDSC proteins was carried out using candidate protein-lists selected on the basis of significantly increased or decreased spectral counts, i.e. proteins with ratio of spectral counts (Rsc) $\geq 1$ and Fisher's exact test FDR $\leq 5\%$ (Benjamini-Hochberg multiple-test correction[126]) with respect to INF or CON MDSC. The same pathway enrichment

analysis was carried out on the ubiquitinated subset of INF and CON MDSC exosome proteins. The set of all identified MDSC exosome proteins was used as the pathway enrichment background for differentially abundant INF and CON proteins, while the set of all ubiquitinated MDSC exosome proteins was used as the pathway enrichment background for differentially abundant ubiquitinated INF and CON proteins. Fisher's exact test and Benjamini-Hochberg FDR, was used to assess the statistical significance of the number of proteins in common between each canonical pathway and the various candidate protein-lists versus the number expected, based on the background protein set.

Spectral counting for identified proteins was carried out using in house software. The spectral count ratios ($R_{SC}$) were generated by the method described in Old et al.[127] The Fisher exact-test was used to generate p-values for differential spectral counts and Benjamini-Hochberg FDR estimates were used to correct for multiple testing.[126]

Spectra of both ubiquitinated and non-ubiquitinated peptides were counted to assess ubiquitinated proteins in this bottom up study. The $R_{SC}$ is reported as the $\log_2$ ratio of INF vs CON exosomes.

### *3.2.4. Bioassay for MDSC Chemotaxis*

As previously reported[128] inflammatory MDSC ($1x10^6$) in 100 µL migration medium (IMDM supplemented with 3% fetal calf serum) were placed in the upper chamber of a 8.0µl transwell and either 500 µL of fresh medium, 500 µL of medium from cultured tumor cells (conditioned medium; positive control), exosomes, exosomes plus 3 µL polyclonal rabbit anti-ubiquitin antibody (ThermoFisher PA1-10023) or 3 µL of an irrelevant polyclonal rabbit antibody inactivated by heating at 56ºC for 30 min (Cederlane, Burlington NC) in the lower chamber. Assembled transwells were incubated for 2 hours at 37°C in air supplemented with

5% $CO_2$.The number of MDSC migrating to the bottom chamber was quantified by hemocytometer. Values for each sample are the average results of triplicate samples and two independent hemocytometer counts per sample.

## *Section 3.3 Results and Discussion*

### *3.3.1 Ubiquitinated proteoforms identified*

Protein cargoes of exosomes derived from mice with low (CON) and high (INF) inflammation were examined using bottom-up mass spectrometry. In this study we have identified a total of 1188 proteins in MDSC exosomes. More than 50% of the proteins identified from both conditions have ubiquitinated proteoforms. The INF MDSC exosome lysate identified 1092 proteins (Appendix 3.1), of which 589 had ubiquitinated proteoforms identified. A protein identified with a GG-modified peptide is one that can be said to have a ubiquitinated proteoform. The CON exosome lysate had 925 proteins identified, and 484 of these contributed ubiquitinated proteoforms (Appendix 3.2).

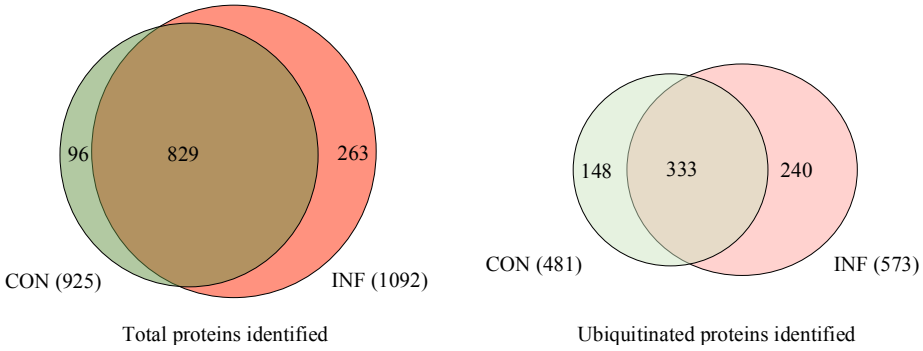


**Figure 3.2.** Venn diagrams of the overlap between proteins in (a) overall proteins identified in CON and INF exosomes and (b) proteins with ubiquitinated proteoforms in CON and INF exosomes.

The overlap between the proteins identified in INF and CON lysates is large, since 90% of the proteins identified in the CON lysate and 76% of the proteins identified in the INF lysate are identified in both conditions (Figure 3.2a). However, the overlap between the ubiquitinated proteins from the same exosome lysates is lower. Figure 3.2(b) shows that only 69% of the Ub proteins identified in the CON lysate and 58% of the Ub proteins in the INF lysate are identified in exosomes from both conditions. A previous study also reported identifying 54 ubiquitinated proteins from MDSC exosomes using immunoprecipitation.[44] We have greatly expanded the number of ubiquitnated proteins identified by using the current strategy of not using enrichment and using the latest generation of Orbitrap mass spectrometers. It is interesting to note that the two strategies of identifying Ub proteins are complementary to each other and only identified 15 Ub proteins in common, and therefore the overall total number of Ub proteins in MDSC exosomes stands at 753.

Several other studies have also found exosomes to be carrying a highly ubiquitinated protein cargo.[39,121] Huebner et al have reported 747 ubiquitinated peptides from 593 proteins in urinary tract exosomes. Our study also finds Ub proteins with more than one site of ubiquitination. Overall, 737 ubiquitinated proteins were identified with 2322 sites of

attachment. More than 50% of these GG-modified tryptic peptides have the GG-modification located on the terminal lysine residue. The terminal GG-modification has been observed by several studies,[39,44,55,129] and a mechanism for such a miscleavage has been proposed.[130]

This study also confirms the presence of polyUb side chains in both CON and INF exosomes (Table 3.1). Tryptic peptides from ubiquitin were identified with GG-addition on K-6, K-11, K-33, K-48 and K-63 residues.

**Table 3.1.** Tryptic GG-modified peptides identified from the protein ubiquitin.

| GG-modified peptide | Residue on Ub | Found in | |
|---|---|---|---|
| MQIFVK$_{(GG)}$TLTGK | K-6 | INF | |
| TLTGK$_{(GG)}$TITLEVEPSDTIENVK | K-11 | INF | CON |
| IQDK$_{(GG)}$EGIPPDQQR | K-33 | INF | CON |
| LIFAGK$_{(GG)}$QLEDGR | K-48 | INF | CON |
| TLSDYNIQK$_{(GG)}$ESTLHLVLR | K-63 | INF | CON |

To determine if ubiquitinated proteins present in MDSC exosomes are biologically functional, a migration assay was performed (Figure 3.3). The hypothesis was based on previous studies which demonstrated that MDSC derived exosomes facilitate the migration of parental MDSC.[7,13,15] Migration was assessed by quantifying the number of parental MDSC that move via chemotaxis through a semi-permeable membrane toward a suspension of MDSC-derived exosomes. Ubiquitin in exosomes was blocked using an anti-Ub antibody, and thus the effect of Ub on MDSC chemotaxis was ascertained. Conditioned media containing exosomes and soluble proteins (a positive control), or purified MDSC-derived exosomes promoted MDSC chemotaxis. However, when exosomes were incubated with anti-Ub antibody, chemotaxis was decreased to a statistically significant extent. Treatment of MDSC derived exosomes with irrelevant control antibody had no effect on chemotaxis. These

results suggest that apparent Ub molecules carried by MDSC-derived exosomes are involved in MDSC chemotaxis.

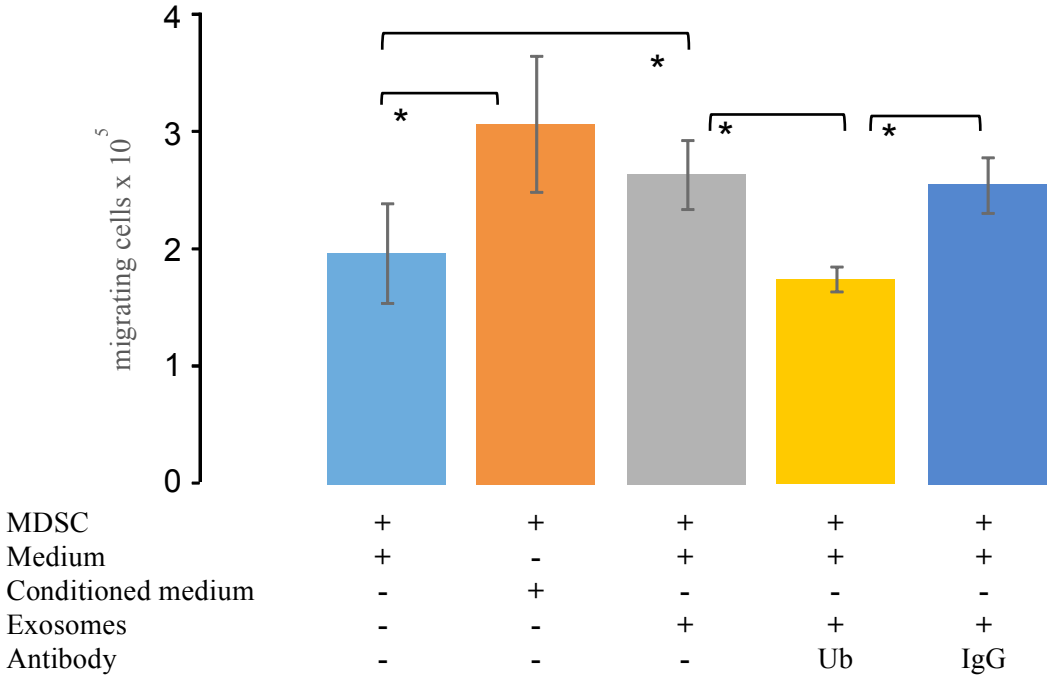


*** Indicates values that are statistically different by at least p<0.004; Standard deviations are shown. Plot is from one of six independent experiments**

**Figure 3.3.** Assay for chemotactic activity in ubiquitinated proteins in exosomes shed by MDSC. MDSC were placed in the upper compartment of transwells and either tumor-conditioned medium or MDSC-shed exosomes ± antibodies to ubiquitin was placed in the lower compartment. The number of MDSC migrating to the lower compartment was determined by hemocytometry after 3 h of incubation.

Previous studies have reported identifying the proinflammatory proteins S100A8 and S100A9 in MDSC exosomes.[7] S100A8 and S100A9 have been shown to create an autocrine feedback loop, which results in sustained accumulation of MDSC. The S100A8 and S100A9 in MDSC exosomes were shown to be biologically active and responsible for MDSC chemotaxis. In this study, S100A8 and S100A9 were identified in CON and INF MDSC exosomes with ubiquitinated proteoforms (Table 3.2).

**Table 3.2.** GG-tagged peptides from proinflammatory cytokines identified in MDSC

| Accession No. | Protein | Peptide | Peptide Spectral Matches (INF/CON) |
|---|---|---|---|
| **P27005** | Protein S100-A8 | [1]MPSELEK(gg)ALSNLIDVYHNYSNIQGNHHALYK | 1/0 |
| | | [8]ALSNLIDVYHNYSNIQGNHHALYK(gg) | 2/2 |
| | | [36]K(gg)MVTTECPQFVQNINIENLFR | 4/4 |
| | | [57]ELDINSDNAINFEEFLAMVIK(gg)VGVASHK | 3/0 |
| **P31725** | Protein S100-A9 | [3]NK(gg)APSQMER | 1/0 |
| | | [37]EFRQMVEAQLATFMK(gg) | 1/2 |
| | | [54]RNEALINDIMEDLDTNQDNQLSFEECMMLMAK(gg)L | 23/14 |
| | | [88]IFACHEK(gg)LHENNPR | 1/0 |

Proteomic studies performed on parental MDSC highlighted other proteins that had a role in the immunosuppressive functionality of MDSC.[17] Chornoguz et al identified proteins involved with Fas-mediated apoptosis and the caspase network in MDSC lysates. INF MDSC was shown to be resistant to Fas-mediated apoptosis, which encourages their accumulation and thus increases their potency. Proteins caspase 3, caspase 8, lamin B1 and Rho GDP inhibitor beta which are associated with the Fas-pathway were identified in parental MDSC.[17] CON and INF MDSC exosomes in this study were also shown to carry proteins from the Fas-pathway. These include caspase-3, caspase-6, Lamin B1, and Rho GDP inhibitor beta

proteins. Further experiments are needed to determine whether MDSC exosomes are carrying a cargo that aids in enabling the INF MDSC to resist Fas-mediated apoptosis.

*3.3.2. The effect of inflammation on ubiquitination*

In this study we used label free spectral counting to examine the effect of inflammation on abundances of the ubiquitinated proteins in the MDSC- derived exosomes. The ubiquitome was compared to the total proteome and the proteins identified without an ubiquitinated peptide. Ratios of spectral counts ($\log_2$ [$R_{SC}$ INF/CON]) are summarized in Figure 3.4. All identified peptides (including GG-modified) were counted for all identified proteins. There were not enough GG-modified peptides identified to use spectral counting with statistical significance and draw conclusions about only the ubiquitinated proteoforms of the proteins identified. Therefore, these results can only be used to draw conclusions about the proteins at an overall level and we cannot distinguish the abundance of specifically the ubiquitinated proteoforms of identified proteins.

The histograms in figure 3.4A and 3.4B show distributions of $R_{SC}$ which are similar for the ubiquitinated proteins and the non ubiquitinated proteins identified in the CON and INF exosomes. However, there is a small bias towards higher $R_{SC}$ in the non ubiquitinated proteins cohort (Figure 3.4B).

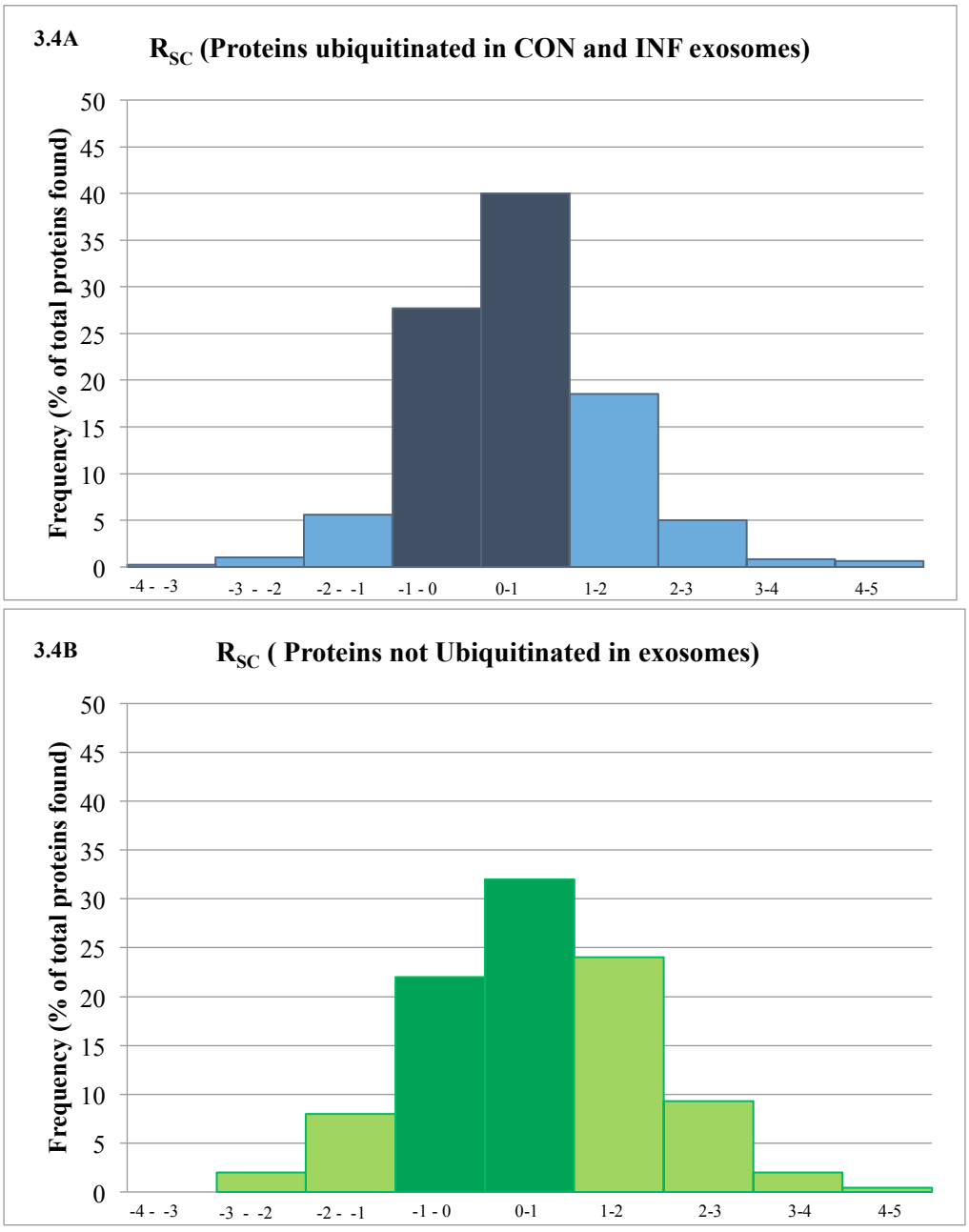


**Figure 3.4.** Histograms of INF/CON ratios of spectral counts ($\log_2$ Rsc) for (a) 753 proteins with ubiquitinated peptides in INF and CON exosomes; (b) 451 proteins for which no GG-tagged peptides were identified. The dark blue and dark green histograms represent the proteins with Rsc between -1 and 1, which are not changed in abundance.

To look further for effects of inflammation, gene ontology was used to compare ubiquitinated cohorts to each other, to the two exosome lysate inventories, and to the non-ubiquitinated proteins. Subcellular location GO annotations (Figure 3.5) show little difference between ubiquitinated proteins in CON and INF samples, between these and proteins in the lysates, and also the non-ubiquitinated cohort of proteins.

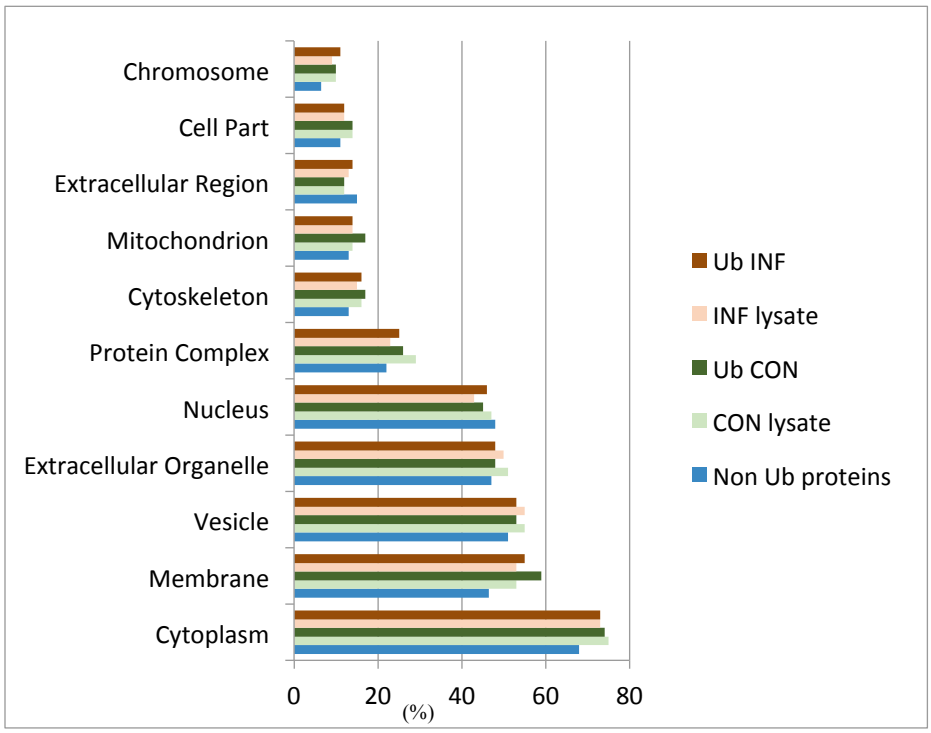


**Figure 3.5.** GO annotation comparisons of subcellular fractions of the INF and CON lysates, the ubiquitinated protein cohorts of two conditions, and the proteins identified without any Ub proteoforms.

Pathway enrichment analysis was carried out using proteins identified in the INF and CON MDSC derived- exosomes. The 1188 proteins identified in CON and INF exosomes were used as the background protein-list, and proteins in the CON and INF exosomes were examined to find statistically increased, or decreased enriched pathways using Fisher's exact test at 10 % FDR. Nine pathways were found to be decreased in the INF cohort of proteins (or increased in CON exosomes) (Table 3.3). The pathways found to have a decreased

presence with an increase in inflammation, are all related to translation and RNA processing. However, no pathways were found to be increased in the INF cohort with statistical significance. A similar analysis was carried out on the ubiquitinated proteins identified in CON and INF exosomes, with the total 753 ubiquitinated proteins identified as the background. However, for this search, no pathways were found to be enriched with statistical significance.

**Table 3.3.** Pathways with a significant decrease in proteins in response to INF. (Note: No pathways were found with a significant increase in response to INF)

| Pathway Description | #Proteins found in CON | #Proteins total in pathway | FDR |
|---|---|---|---|
| SRP-dependent cotranslational protein targeting to membrane | 8 | 98 | 8.6691E-08 |
| Nonsense Mediated Decay (NMD) independent of the Exon Junction Complex (EJC) | 8 | 95 | 1.12946 E-07 |
| Nonsense Mediated Decay (NMD) enhanced by the Exon Junction Complex (EJC) | 8 | 120 | 2.98042 E-07 |
| Formation of a pool of free 40S subunits | 8 | 103 | 1.03459 E-06 |
| L13a-mediated translational silencing of Ceruloplasmin expression | 8 | 112 | 1.78955 E-06 |
| GTP hydrolysis and joining of the 60S ribosomal subunit | 8 | 114 | 2.12839 E-06 |
| Formation of the ternary complex, and subsequently, the 43S complex | 6 | 53 | 2.38644 E-05 |
| Translation initiation complex formation | 6 | 59 | 2.89624 E-05 |
| Ribosomal scanning and start codon recognition | 6 | 60 | 3.49053 E-05 |

Hundreds of ubiquitinated proteins have been identified in MDSC derived exosomes. Other studies have reported identifying a large cargo of ubiquitinated proteins in exosomes.[39,121] Also, the role of extracellular Ub in modulating immune responses has been reported. The next section will highlight enzymes identified in INF and CON exosomes that are involved in the Ub signaling system and could therefore shed light into possible roles of ubiquitinated proteins in MDSC-derived exosomes.

*Ubiquitin-utilizing enzymes*

Three families of ubiquitin-utilizing enzymes have been identified in the protein lysates of CON and INF exosomes. The first family identified is enzymes involved in the ubiquitin- conjugating pathway (Table 3.4). Ubiquitin- activating enzyme E1 activates the conjugation of Ub in eukaryotic cells. Ubiquitin conjugating enzyme E2 N catalyzes the synthesis of poly-Ub chains that are linked through K63s and are implicated in the regulation of Toll-like, NOD-like, and RIG-l-like inflammatory pathways.[115] Of the several hundred available E3 type ligases, four were identified in this study. One of these, E3 ubiquitin-protein ligase UBR4 (A2AN08), is reported to form meshwork structures with clathrin (also identified in MDSC exosomes) and may be involved in invagination.[131]

Eight deubiquitinase enzymes were also identified in the lysate of INF and CON exosomes (Table 3.5). Ubiquitin terminal hydrolase 15 has been implicated in immune response modulation by the inactivation of T-cell responses. The relative abundances of Ub ligases and hydrolases are similar in INF and CON exosomes

**Table 3.4.** Enzymes involved in the ubiquitin conjugation pathway.

| Accession No. | Protein | Distinct Spectral Counts INF(-gg)* | Distinct Spectral Counts CON(-gg)* |
|---|---|---|---|
| Q02053 | Ubiquitin-activating enzyme E1 | 395(6) | 286(3) |
| P68037 | Ubiquitin-conjugating enzyme E2 L3 | 32(0) | 7(0) |
| P61089 | Ubiquitin-conjugating enzyme E2 N | 6 | 3 |
| P22682 | E3 ubiquitin-protein ligase CBL | 1(1) | 0 |
| A2AN08 | E3 ubiquitin-protein ligase UBR4 | 13(6) | 22(5) |
| Q6PAV2 | Probable E3 ubiquitin-protein ligase HERC4 | 4(1) | 1 |
| O08759 | Ubiquitin-protein ligase E3A | 2(1) | 0 |
| Q9D906 | Ubiquitin-like modifier-activating enzyme 1 | 27(1) | 30(2) |
| Q8C7R4 | Ubiquitin-like modifier-activating enzyme 6 | 2 | 1 |

* Entries in parenthesis indicate the number of GG-tagged peptides identified.

**Table 3.5.** Enzymes involved in hydrolysis of ubiquitin.

| Accession No. | Protein | Distinct Spectral Counts INF(-gg*) | Distinct Spectral Counts CON(-gg*) |
|---|---|---|---|
| Q9JMA1 | Ubiquitin carboxyl-terminal hydrolase 14 | 25(2) | 10(2) |
| P70398 | Probable ubiquitin carboxyl-terminal hydrolase FAF-X | 20(6) | 35(2) |
| P56399 | Ubiquitin carboxyl-terminal hydrolase 5 | 27(2) | 27(3) |
| Q7TQI3 | Ubiquitin thioesterase OTUB1 | 17 | 16 |
| Q6A4J8 | Ubiquitin carboxyl-terminal hydrolase 7 | 56 | 36(1) |
| Q8R5H1 | Ubiquitin carboxyl-terminal hydrolase 15 | 5(3) | 4(1) |
| B1AY13 | Ubiquitin carboxyl-terminal hydrolase 24 | 5(2) | 6(3) |
| Q9WUP7 | Ubiqui tin carboxyl-terminal hydrolase isozyme L5 | 8 | 2 |

* Entries in parenthesis indicate the number of GG-tagged peptides identified.

The 26S proteasome is a protein family that hydrolyses Ub conjugates and has been identified in exosomes in other studies. Thirty-seven known subunits make up the murine proteasome and immunoproteasome. In this study we have identified 33 out of these 37 subunits (Table 3.6). Six other proteomics studies have identified subunits of the 26S proteasome in exosomes derived from murine and human cells.[39,42,132–135] Proteolytic activity of the 26S proteasome has been demonstrated in the lysate of exosomes derived from tumor associated macrophages and in the exosomes derived from mesenchymal stem cells.[132,134] The proteasome has been shown to help regulate cytokine induction and to activate NF-κB, maintaining an inflammatory environment which exacerbates the immunosuppressive effect of MDSC.[136,137]

**Table 3.6.** Proteasome subunits identified and ratios of spectral counts calculated.

| Accession | Protein Name | Distinct Spectral Counts INF(-gg*) | Distinct Spectral Counts CON (-gg*) |
|---|---|---|---|
| Q3TXS7 | 26S proteasome non-ATPase regulatory subunit 1 | **125(29)** | **127(26)** |
| Q8BG32 | 26S proteasome non-ATPase regulatory subunit 11 | **55(1)** | 47 |
| Q9D8W5 | 26S proteasome non-ATPase regulatory subunit 12 | 28 | 62 |
| Q9WVJ2 | 26S proteasome non-ATPase regulatory subunit 13 | 73 | 42 |
| O35593 | 26S proteasome non-ATPase regulatory subunit 14 | **64(1)** | **61(3)** |
| Q8VDM4 | 26S proteasome non-ATPase regulatory subunit 2 | **250** | **213** |
| P14685 | 26S proteasome non-ATPase regulatory subunit 3 | 62 | 43 |
| O35226 | 26S proteasome non-ATPase regulatory subunit 4 | **1(1)** | 4 |
| Q8BJY1 | 26S proteasome non-ATPase regulatory subunit 5 | **26(2)** | **25(2)** |
| Q99JI4 | 26S proteasome non-ATPase regulatory subunit 6 | **60(1)** | **59(1)** |
| P26516 | 26S proteasome non-ATPase regulatory subunit 7 | 68 | 68 |
| Q9CX56 | 26S proteasome non-ATPase regulatory subunit 8 | **6(1)** | **8(3)** |
| P46471 | 26S protease regulatory subunit 7 | 50 | **51(1)** |
| P62192 | 26S protease regulatory subunit 4 | 22 | **57(2)** |
| P62334 | 26S protease regulatory subunit 10B | 43 | **50(1)** |
| O88685 | 26S protease regulatory subunit 6A | **77(2)** | 109 |
| P62196 | 26S protease regulatory subunit 8 | **37(2)** | **37(1)** |
| Q9R1P4 | Proteasome subunit alpha type-1 | 101 | 64 |
| P49722 | Proteasome subunit alpha type-2 | **198(3)** | 208 |
| O70435 | Proteasome subunit alpha type-3 | 71 | 90 |
| Q9R1P0 | Proteasome subunit alpha type-4 | **106(2)** | 37 |
| Q9Z2U1 | Proteasome subunit alpha type-5 | **149(3)** | **105(3)** |
| Q9QUM9 | Proteasome subunit alpha type-6 | **99(2)** | **117(3)** |
| Q9Z2U0 | Proteasome subunit alpha type-7 | 120 | 84 |
| O09061 | Proteasome subunit beta type-1 | **176(2)** | **144(1)** |
| Q9R1P3 | Proteasome subunit beta type-2 | 143 | 89 |
| Q9R1P1 | Proteasome subunit beta type-3 | **65(1)** | **66(1)** |
| P99026 | Proteasome subunit beta type-4 | 138 | **136(1)** |
| *O55234* | *Proteasome subunit beta type-5* | *37* | *22* |
| *Q60692* | *Proteasome subunit beta type-6* | ***96(1)*** | ***57(1)*** |
| *P70195* | *Proteasome subunit beta type-7* | ***104(1)*** | ***57(1)*** |
| *O35955* | *Proteasome subunit beta type-10* | ***22(1)*** | *27* |
| *P28063* | *Proteasome subunit beta type-8* | *84* | *72* |
| *P28076* | *Proteasome subunit beta type-9* | ***50(1)*** | ***32(1)*** |

† Italics indicate the subunit belongs uniquely to the immunoproteasome.

* Entries in parenthesis indicate the number of GG-tagged peptides identified.

The final ubiquitin-utilizing family identified in MDSC exosomes is proteins from the ATP glycolysis pathway (Table 3.7). This enzyme family has previously been identified in exosomes derived from mesenchymal stem cells and prostate cells.[133,138] Exosomes from prostate cells have been confirmed to synthesize ATP.[138] It could be possible that these enzymes in MDSC exosomes derive the ATP required for Ub conjugation.

**Table 3.7.** Proteins identified from the ATP glycolysis pathway.

| Accession | Protein Name | Distinct Spectral Counts INF(-gg)* | Distinct Spectral Counts CON(-gg)* |
|---|---|---|---|
| P16858 | glyceraldehyde 3-phosphate dehydrogenase | 800(1) | 1273(2) |
| P09411 | phosphoglycerate kinase | 219(3) | 151(4) |
| Q9DBJ1 | phosphoglycerate mutase | 133(1) | 56(2) |
| P17182 | Enolase I aka alpha enolase | 659(1) | 920(2) |
| P52480 | pyruvate kinase | 749(1) | 1639(2) |

## *Section 3.4 Conclusions*

This bottom-up analysis of the protein cargo of MDSC-derived exosomes finds that more than 60% of the identified proteins contribute a ubiquitinated proteoform. Averages of three sites of ubiquitination are reported per protein identified. The number of sites of ubiquitination per proteoform is not known, but could be determined by a follow-up top-down mass spectrometry analysis of the protein cargo. Migration bioassays demonstrate that ubiquitinated proteins carried by the MDSC-derived exosomes contribute to MDSC chemotaxis.

No significant differences were seen in the histogram distribution of Rsc values and subcellular GO annotations of ubiquitinated and non-ubiquitinated cohorts of proteins. The pathway enrichment analysis using REACTOME database was indicative of increased inflammation being independent of the ubiquitination in exosomes. It was found that an increase of inflammation leads to the decrease in proteins associated with translation and RNA processing in MDSC-derived exosomes. However, it remains unclear which pathways are enriched as inflammation is increased. Perhaps, the pathways involved are not yet annotated in the REACTOME database.

The current study has identified proteins from the enzyme families E1, E2, and E3, which are required for ubiquitination. In addition, nine Ub-hydrolases have also been identified in INF and CON exosomes. The presence of enzymes for ATP synthesis, and a majority of the 26S proteasome have also been confirmed to be carried by the MDSC-derived exosomes. Studies by other labs have confirmed the intra-exosomal activity of the glycolytic enzymes and the 26S proteasome. The identification of these protein families leads to the hypothesis that ubiquitination is a modification which could be self-established in the MDSC-derived exosomes. In summary, the MDSC-derived exosomes carry a large cohort of ubiquitinated proteins, and the machinery to generate the modification of ubiquitination within the MDSC-derived exosomes. It is currently not evident that an increased inflammatory environment has an effect on the ubiquitination observed in the MDSC-derived exosomes.

# Chapter 4: Top-down analysis of ubiquitinated proteins in MDSC-derived exosomes

*Introduction*

The ubiquitome of the MDSC exosomes has been interrogated using bottom-up mass spectrometry in Chapter 3 of this thesis. Our study reported that the MDSC-derived exosomes are hyperubiquitinated, as over 60% of the 1188 proteins were identified with GG-modified peptides. Also, ubiquitinated proteins were identified with an average of 3 sites of ubiquitination. While our bottom-up strategy provides insight into how many proteins are ubiquitinated and the site of ubiquitination on the substrate protein, it is limited in its ability to discern the topology of the ubiquitin chain on the substrate protein. Bottom-up proteomics is also limited in its ability to determine whether a protein has several sites of ubiquitination or whether there are several isoforms of the same protein with varied Ub linkage sites.

An alternative approach to bottom-up proteomics is the use of top-down proteomics to study ubiquitination. Top-down mass spectrometry involves the study of the protein without digesting it to form peptides. The whole protein is kept intact when introduced into the mass spectrometer, which allows the identification of post-translation modifications on the protein. Top-down proteomics has been established as a tool for discerning different linkages and topologies of polyubiquitin.[53,54] Using the enhanced capabilities of ETD fragmentation on the orbitrap Fusion Lumos mass spectrometer, high sequence coverage of polyubiquitins has been achieved. Optimization of fragmentation conditions has led to being able to detect ions unique to a specific linkage and/or topology of polyubiquitin chains.[53,54]

Our current study will extend these methods, which were developed on chemically, and enzymatically synthesized polyubiquitin dimers, trimers and tetramers, to find endogenous Ub conjugates in a complex biological sample. Since the MDSC-derived exosomes have been shown to carry over 700 proteins with ubiquitin proteoforms, they make a good candidate for the extension of the top-down strategy to characterize polyubiquitins. We hypothesize that using top-down mass spectrometry, polyubiquitin and ubiquitinated proteins will be identified and their linkage and topology can be determined in MDSC-derived exosomes.

Currently, top-down proteomics allows for characterization of proteins up to 30 kDa in mass using an unmodified high-resolution orbitrap mass spectrometer.[139] This means that Ub trimers (27 kDa) in a complex mixture of proteins can be easily detected. However, in order to detect Ub tetramers (34 kDa), a fractionated / simplified mixture of proteins will aid in the mass spectrometric identification. Ubiquitin conjugation provides a large mass change of 8.5 kDa. Therefore, monoubiquitinated proteins can have a maximum mass of 21.5 kDa to be routinely detected using the orbitrap mass analyzer. For routine analysis of polyubiquinated proteins, the substrate protein can weigh a maximum of 13 kDa since the addition of a Ub dimer (17 kDa) will bring the total mass to 30kDa. In the current list of 776 ubiquitinated proteins we have 69 proteins under 21.5 kDa, which would make good candidates for top-down characterization from the MDSC-derived exosomes (Table 4.1). It is possible that other proteins are also ubiquitinated in exosomes but were not identified in the bottom-up study. Peptides from the ubiquitin protein were identified with a GG-modification at lysine residues (Table 3.1), which indicates the presence of polyubiquitins in the MDSC-exosome lysate. Other studies report that exosomes carry a cargo of mostly monoubiquitinated proteins, which would make a top-down analysis feasible.[140]

In the current study MDSC-derived exosomes will be lysed and purification of Ub conjugates will be attempted. Proteins will be analyzed by a high-resolution orbitrap mass spectrometer, and class characteristic fragment ions from ubiquitin will be searched for in the reconstructed ion chromatogram. The raw data will also be analyzed using the bioinformatics platform Proteome Discoverer to identify ubiquitinated proteins.

**Table 4.1.** Ubiquitinated proteins identified in bottom up analysis of exosomes which weigh less than 21.5 kDa without the ubiquitin side chain.

| **Accession number** | **Protein Name** | **M.wt (Da)** |
|---|---|---|
| P62843 | 40S ribosomal protein S15 | 16908.91 |
| P63276 | 40S ribosomal protein S17 | 15392.89 |
| P47955 | 60S acidic ribosomal protein P1 | 11343.71 |
| P99027 | 60S acidic ribosomal protein P2 | 11650.91 |
| P35979 | 60S ribosomal protein L12 | 17804.56 |
| B1ATY1 | Actin, cytoplasmic 2 | 16734.34 |
| Q9JM76 | Actin-related protein 2/3 complex subunit 3 | 20393.49 |
| P59999 | Actin-related protein 2/3 complex subunit 4 | 19535.82 |
| P11031 | Activated RNA polymerase II transcriptional coactivator p15 | 14296.25 |
| P84078 | ADP-ribosylation factor 1 | 20565.58 |
| P84084 | ADP-ribosylation factor 5 | 20398.46 |
| P31230 | Aminoacyl tRNA synthase complex-interacting multifunctional protein 1 | 17989.88 |
| O54962 | Barrier-to-autointegration factor | 10102.59 |
| Q63810 | Calcineurin subunit B type 1 | 19168.72 |
| P60766 | Cell division control protein 42 homolog | 20933.16 |
| P18760 | Cofilin-1 | 18428.35 |
| P45591 | Cofilin-2 | 18578.4 |
| P63242 | Eukaryotic translation initiation factor 5A-1 | 16701.06 |
| P09528 | Ferritin heavy chain | 20935.41 |
| P09528 | Ferritin heavy chain | 21066.6 |
| Q8K0E8 | Fibrinogen beta chain | 1697.64 |

| | | |
|---|---|---|
| Q9ERL7 | Glia maturation factor gamma | 16617.13 |
| Q61646 | Haptoglobin precursor | 9468.57 |
| Q9R257 | Heme-binding protein 1 | 21066.85 |
| P01942 | Hemoglobin subunit alpha | 14953.98 |
| P02088 | Hemoglobin subunit beta-1 | 15708.99 |
| P02089 | Hemoglobin subunit beta-2 | 15747.06 |
| P15864 | Histone H1.2 | 21135.46 |
| Q8CGP4 | Histone H2A | 14056.35 |
| C0HKE5 | Histone H2A type 1-G | 14004.3 |
| Q6GSS7 | Histone H2A type 2-A | 13964.3 |
| P0C0S6 | Histone H2A.Z | 13421.55 |
| P27661 | Histone H2AX | 15011.41 |
| P10854 | Histone H2B type 1-M | 13804.97 |
| Q8CGP0 | Histone H2B type 3-B | 13776.92 |
| F8WI35 | Histone H3 | 15198.8 |
| P68433 | Histone H3.1 | 15272.89 |
| P84228 | Histone H3.2 | 15256.83 |
| P84244 | Histone H3.3 | 15196.72 |
| P62806 | Histone H4 | 11236.15 |
| A0A0A6YYE5 | Immunoglobulin kappa variable 4-78 | 10348.47 |
| B2RV77 | MCG130182, isoform CRA_a | 10965.57 |
| Q6ZWQ9 | MCG5400 | 19895.3 |
| P11247 | Myeloperoxidase | 13005.71 |
| Q60605 | Myosin light polypeptide 6 | 16798.86 |
| Q3THE2 | Myosin regulatory light chain 12B | 19779.16 |
| Q9CQ19 | Myosin regulatory light polypeptide 9 | 19723.02 |
| O08692 | Neutrophilic granule protein | 17141.98 |
| P09602 | Non-histone chromosomal protein HMG-17 | 9291.5 |
| P24369 | Peptidyl-prolyl cis-trans isomerase B | 20218.15 |
| P99029 | Peroxiredoxin-5, mitochondrial | 17014.79 |

| | | |
|---|---|---|
| P0CG50 | Polyubiquitin-C | 8564.84 |
| P62962 | Profilin-1 | 14826.02 |
| O54824 | Pro-interleukin-16 | 12219.78 |
| P28076 | Proteasome subunit beta type-9 | 21326.22 |
| Q99LX0 | Protein DJ-1 precursor | 19890.11 |
| P14069 | Protein S100-A6 | 10050.62 |
| P27005 | Protein S100-A8 | 10163.4 |
| P31725 | Protein S100-A9 | 12917.67 |
| P63001 | Ras-related C3 botulinum toxin substrate 1 | 21110.63 |
| P84096 | Rho-related GTP-binding protein RhoG | 20969.03 |
| Q99KH8 | Serine/threonine-protein kinase 24 | 12699.31 |
| Q9JI10 | Serine/threonine-protein kinase 3 | 20367.52 |
| Q9JI11 | Serine/threonine-protein kinase 4 | 18458.7 |
| P62315 | Small nuclear ribonucleoprotein Sm D1 | 13281.57 |
| P62320 | Small nuclear ribonucleoprotein Sm D3 | 13785.05 |
| Q9ESP1 | Stromal cell-derived factor 2-like protein 1 | 20899.07 |
| P10639 | Thioredoxin | 11544.25 |
| Q9QZ88 | Vacuolar protein sorting-associated protein 29 | 20495.69 |

## *4.2. Methods*

### *4.2.1. Myeloid-Derived Suppressor Cells and Exosome harvesting*

Female BALB/c mice, 6-10 weeks of age (bred in the UMBC animal facility from breeding pairs obtained from The Jackson Laboratory, Bar Harbor, ME), were injected in the mammary fat pad with 7000 4T1 cells transfected with the IL-1β gene (4T1/IL-1β) cells. Mice were bled from the submandibular vein when tumors were greater than 8mm in diameter. MDSC were harvested from the blood, labeled with fluorescently coupled antibodies to MDSC markers, and assessed by flow cytometry (Beckman/Coulter Cyan ADP) for purity.[7,17] Cell populations that were >90% pure $Gr1^{+}CD11b^{+}$ cells were used in these studies. Approximately $10^{8}$ MDSC were obtained from 2-3 mice. Following isolation from mice, MDSC were maintained in serum-free HL-1 media overnight at 37°C to collect exosomes. 20. After 18 hr each supernatant containing exosomes was centrifuged at 805xg and 2090xg to remove residual cells and then ultracentrifuged at 100,000xg to pellet the exosomes. Pellets containing the exosomes were resuspended in PBS and they were stored at -80°C with DUBs inhibitors added. Next, several strategies were evaluated to enrich ubiquitinated proteins.

*4.2.2. Ubiquitin proteome enrichment using Tandem Ubiquitin Binding Entities (TUBES)*

Exosomes from $1.6x10^8$ cells were thawed and lysed in TUBES lysis buffer (50 mM Tris-HCl, 0.15 M NaCl, 1 mM EDTA, 1 % Nonidet P-40, 10 % glycerol, pH 7.5), 50 µM deubiquitinase inhibitor PR-619 (LifeSensors, Malvern, PA), 15 µM of deubiquitinase inhibitor MG-132 (Enzo Life Sciences), 10 mM N-ethylmaleimide (Sigma-Aldrich, St. Louis, MO) and 1% of a protease inhibitor cocktail (Sigma-Aldrich, St. Louis, MO). The lysates were centrifuged at 14 000xg for 30 min with a 3 kDa molecular weight cut off filter, and the filtrates were discarded. This process was repeated three times. After lysis of exosomes the buffer was diluted and concentrated in 50 mM ammonium bicarbonate. Protein was collected by inverting the filters and centrifuging at 1000xg for 2 min. Protein content before and after TUBES isolation was measured by the Quick Start Bradford Assay (BioRad, Hercules, CA). The protein lysate was incubated in a spin column (Thermo Fisher Scientist, Waltham, MA) with uncoupled agarose for 30 min at 4°C on a rotator. Agarose TUBES II (100 µl of a 50% slurry)( LifeSensors, Malvern, PA) was added to Poly-prep columns (Bio-Rad, Hercules, CA) and washed three times Tris buffered saline with Tween (TBS-T). The cleared exosome protein lysate was added to the slurry of agarose-TUBEs II. The TUBES-II and exosome lysate was incubated overnight on a rotator at 4°C. The non-bound proteins were collected and the resins were washed 3x with TUBES lysis buffer. Ubiquitinated proteins were eluted by shaking for 5 min on shaker with 2 bead volumes of 1 M NaCl (2x) and 0.2 M glycine pH 2.5 (6x), and with 2 % SDS (2x). The eluted proteins were then desalted with C4 zip-tips (EMD Millipore, Billerica, MA) according to the manufacturer's protocol.

*4.2.3. Immunoprecipitation of Ubiquitinated Proteins Using FK2 Antibody*

Exosomes from $2x10^9$ cells were lysed with RIPA buffer (PBS containing 1% Nonidet P-40, 0.5 % sodium deoxycholate, 0.1 % SDS), 50 μM deubiquitinase inhibitor PR-619 (LifeSensors, Malvern, PA), 15 μM of deubiquitinase inhibitor MG-132 (Enzo Life Sciences), 10 mM N-ethylmaleimide (Sigma-Aldrich, St. Louis, MO) and 1% of a protease inhibitor cocktail (Sigma-Aldrich, St. Louis, MO). They were centrifuged at 14, 000xg for 30 min with a 3 kDa molecular weight cut off filter, and the supernatants were discarded. This process was repeated three times. After lysis, the buffer was diluted to 0.8 M urea in 50 mM ammonium bicarbonate. Protein was collected by inverting the filters and centrifuging at 1000xg for 2 mins. Protein content before and after FK2 immunoprecipitation was measured by the Quick Start Bradford Assay (BioRad, Hercules, CA).

The exosome protein lysate was pre-incubated with control agarose for 1 hour at 4°C on a rotator. The non-bound flow through was collected and incubated with 30 μg of immobilized FK2 antibody. The anti-Ub FK2 antibody (Enzo Lifesciences, Farmingdale, NY) was bound to protein A/G and agarose according to directions provided in the Pierce Crosslink Immunoprecipitation kit column (Thermo Fisher Scientist, Waltham, MA). The precleared lysate and FK2 antibody was incubated overnight on a rotator at 4°C. The non-bound fractions were collected by washing 4x with 10 bead volumes of RIPA buffer. Bound ubiquitinated proteins were eluted from the FK2 antibody using three elution methods- 8M urea buffer (8 M urea, 300 mM NaCl, 50 mM $Na_2HPO_4$, 0.5 % NP-40, pH 8), 2 % SDS and 0.1 % glycine (pH 2). The proteins were incubated with each elution buffer for 5 min on shaker, and then collected by centrifugation 1000xg, 1min at room temperature. This was repeated 3x for each elution buffer.

*4.2.3.1.Western Blot Analysis*

Fractions collected from each step of the FK2-antibody immunoprecipitation were subjected to one-dimensional gel electrophoresis on an 8−16% Criterion precast gel (Bio-Rad, Hercules, CA) at 200 V, 50 mA, and 15 W for 45 min. One-third of each of the fractions collected were run on the gel. Gel electrophoresis was followed by transfer of the proteins to a PVDF membrane (EMD Millipore, Billerica, MA) at 100 V, 250 mA, and 25W for 50 min. Ubiquitin and ubiquitinated proteins were detected by blotting with primary anti-ubiquitin antibody FK2, followed by anti-mouse IgG-HRP (Cell Signaling Technology). Protein bands were visualized using SuperSignal West Dura chemiluminescent substrate (Thermo Fisher Scientific, Waltham, MA) with an Image Lab System (Bio-Rad, Hercules, CA) and Gel-Doc program (Kodak Molecular Imaging Systems).

*4.2.4. Exosome Ubiquitome Analysis Without Enrichment*

Exosomes from $4.9x10^8$ cells were thawed and lysed in 8 M urea in 50 mM Ammonium bicarbonate with 15 μM of deubiquitinase inhibitor MG-132. They were centrifuged at 14 000xg for 30 min with a 3 kDa molecular weight cut off filter, and the supernatants were discarded. This process was repeated three times. After lysis, the buffer was diluted to 0.8 M Urea using 50 mM ammonium bicarbonate in the 3 kDa molecular weight cut off filter. Protein was collected by inverting the filters and centrifuging at 1000g for 2 min. Protein content was measured by the Quick Start Bradford Assay. Proteins were reduced using 10mM TCEP in 0.1 % acetic acid (pH 2) for 15 min at 60 °C. The same lysate was also used for an experiment where different concentrations of K-48 linked linear Ub trimer (Boston Biochemical Inc, Cambridge, MA) were spiked into the lysate, followed by mass spectrometry evaluation. The concentrations of the Ub trimer spike in were- 1% trimer

(10 ng trimer in 1µg of lysate), 2.5% (25 ng trimer in 1µg of lysate), 5% (50 ng trimer in 1µg of lysate), and 20% (200 ng in 1µg of lysate).

*4.2.4.1. Liquid Chromatography Mass Spectrometry Analysis*

Exosome protein lysates (without enrichment) were analyzed using an Ultimate 3000 RSLC nano ultra-high performance liquid chromatograph (Dionex, Sunnyvale, CA). The LC was used in line with the orbitrap Fusion Lumos mass spectrometer (Thermo Fisher Scientific, Waltham, MA). Exosome lysates were desalted and concentrated in a PepSwift RP-4H monolith trap (100 µm × 5 mm) and then separated using a ProSwift RP-4H monolith column (200 µm × 25 cm). Proteins were then separated using a linear gradient from 1−55% B (97.5% acetonitrile, 0.01% formic acid) for 145 min, where solution A is 97.5 % water, 0.01 % formic acid. For some analyses, proteins were desalted and concentrated at 20 % solution B, and separated using a linear gradient from 20-55 % B for 145 min. The mass spectrometer was optimized for intact protein analysis in which the ion routing multipole pressure was maintained at 3 mTorr. Precursor and product ions were analyzed in the orbitrap with mass resolution 120,000. The "Top-speed" data-dependent mode was selected for precursor ions fragmentation in which a maximum number of abundant precursors are isolated by the quadrupole in a fixed duty cycle time of 10s. Precursor ions with a charge state +8 or higher were selected for fragmentation, and precursors with an undetermined charge state were included too. Dynamic exclusion was set to 60 s for this analysis. The fragmentation technique used was EThcD with a reaction time of 6 ms for electron transfer dissociation (ETD) and 10% supplemental higher collision energy (HCD). Three microscans were averaged for each spectrum generated. Automatic gain control targets were set to $1 \times 10^6$ for precursor ions and $5 \times 10^5$ for product ions with a 200 ms maximum injection time.

#### *4.2.4.2. Bioinformatics*

Data processing was performed using the Prosight node v. 1.1 in the Proteome Discoverer v.2.1 suite (Thermo Scientific, San Jose). Each raw data file was searched against the *Mus musculus* database downloaded from the Uniprot database (June 2017). The searches were performed with the following parameters: precursor mass tolerance 40,000 Da, fragment mass tolerance 10 ppm, precursor m/z tolerance of 0.2, max retention time difference 0.5 min, precursor and fragment S/N threshold of 3. The target decoy peptide spectrum match (PSM) validator was used with a maximum delta correlation of 0.05. Only PSMs reported with a high confidence Xcorr score were retained in this study. Prosight Lite was used to view the MS/MS ions identified for the proteins,[141] with a fragment tolerance of 10 ppm. Xcalibur v.2.1. was used to view the raw data and generate extracted ion chromatograms.

## *4.3. Results*

### *4.3.1. TUBES Ubiquitin enrichment*

The goal in this study was to isolate endogenous ubiquitinated proteins from MDSC-derived exosomes and analyze the proteins using top-down mass spectrometry. Three different approaches were evaluated and optimized to this end: (1) agarose-TUBES, (2) anti-Ub antibody FK2, and (3) top-down investigation of non-fractionated exosome lysate. Agarose-TUBES are based on high affinity Ub binding domains which specifically bind to polyUb conjugates.[142] As a proof of concept, agarose-TUBES II (which has an equal affinity for K-48 and K-63 linked polyUb) was used to isolate a synthetic standard mixture of K-48

linear polyUb chains of different lengths (courtesy of Dulith Abyekoon in the laboratory of Dr. David Fushman) (Figure 4.1).

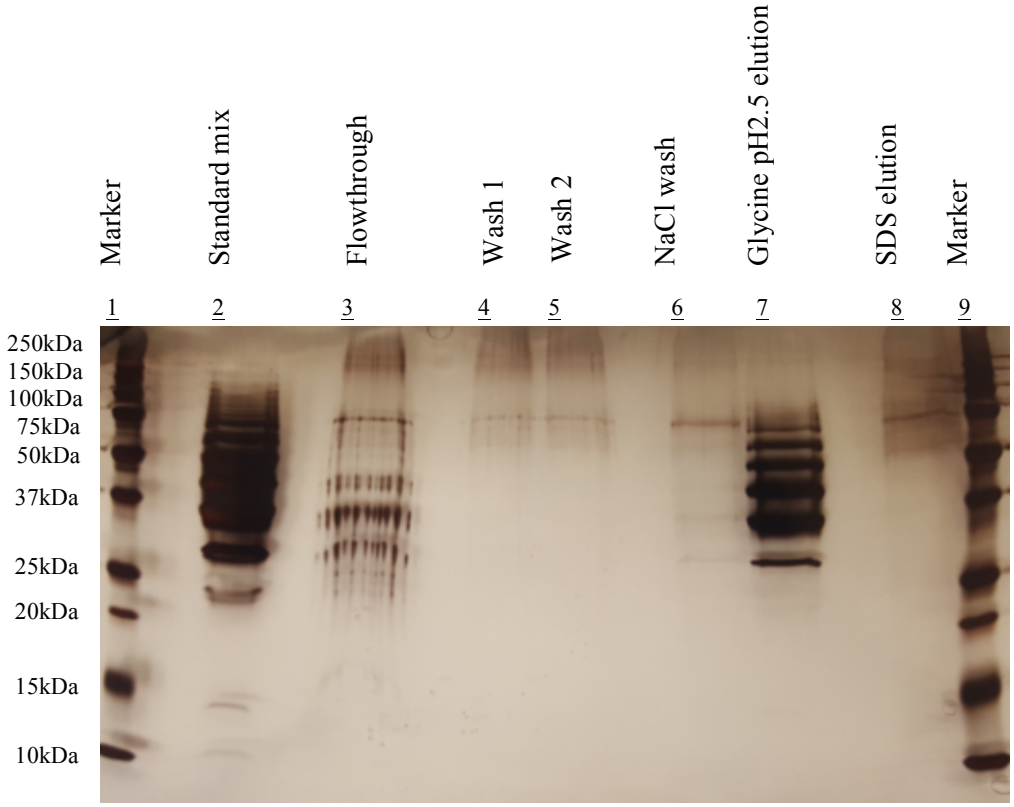


**Figure 4.1.** One-dimensional silver stained gel that depicts the different fractions collected from the agarose-TUBES II enrichment of 10µg of a standard poly Ub mix.

The experiment confirmed the successful use of agarose-TUBES to enrich polyUb conjugates. Lane 2 (Figure 4.1) is the standard polyUb mix run on the gel (without incubation with agarose-TUBES II). Lane 7 is elution of the poly Ub mix post agarose-TUBES II enrichment. The lowest band observed in lane 2 which corresponds to monoUb, was not observed in the lane 7. This is an indication of the specificity of agarose-TUBES II for polyUb conjugates. However, agarose-TUBES II polyUb enrichment from protein in lysates of MDSC-derived exosomes did not yield expected results (Figure 4.2)

.

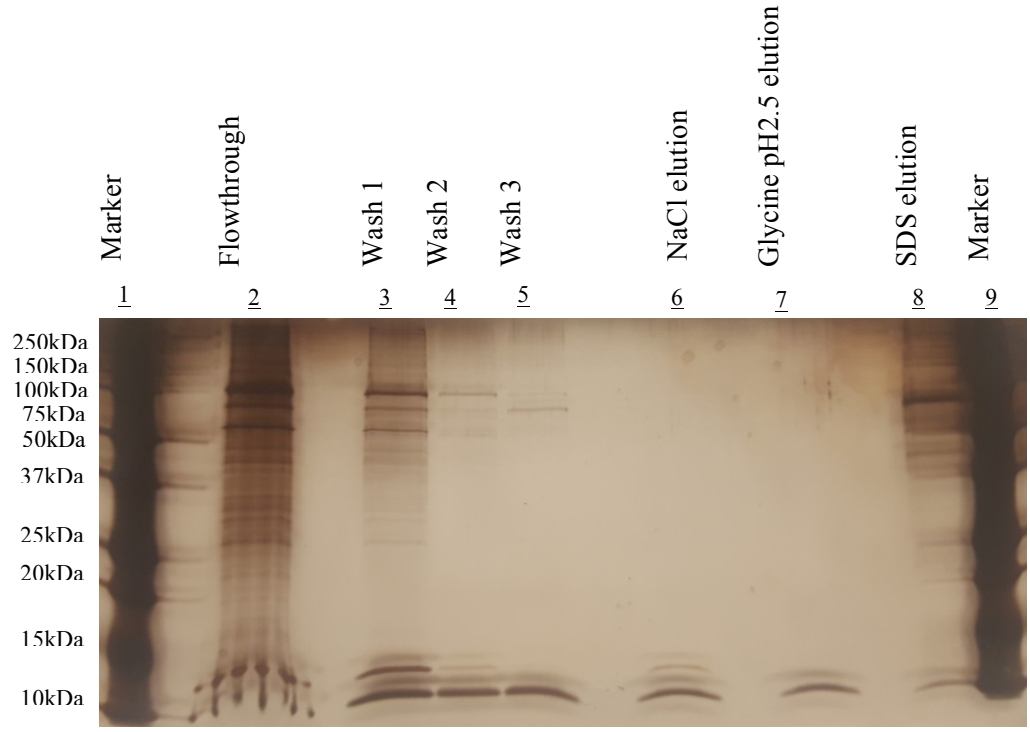


**Figure 4.2.** One-dimensional silver stained gel which depicts the different fractions collected from the agarose-TUBES II enrichment of protein lysate from MDSC-derived exosome.

A band at around 10kDa is observed in the lanes 2-8 in the silver stained gel (Figure 4.2). This mass is too low to be a polyUb protein and is therefore indicative of carryover from the wash steps. No other bands at higher masses were observed from the elution fraction. There are two possibilities for this result- 1. Most proteins in exosomes may exhibit mono ubiquitination or multiple mono ubiquitination, and therefore the agarose TUBES did not enrich the Ub protein conjugates. 2. We may need a higher amount of starting material. Schwertman et al performed a successful purification of polyUb conjugates from HeLa and XP2OS cells using agarose-TUBES.[142] However, Schwertman et al used 5.3 mg of protein lysate from cultured cells whereas this study has limited starting material of ~150 µg from each batch of purified exosomes. Therefore, a second strategy of using anti-Ub antibody FK2 was implemented to enrich for endogenous Ub conjugates from MDSC-derived exosomes.

*4.3.2. Immunoprecipitation using FK2 antibody*

The anti-Ub FK2 antibody was chosen for its ability to enrich mono- and polyUb conjugates. Schertmann et al. had described a detailed optimized protocol for immunoprecipitation using anti-Ub FK2 from cells, which was used in this study.[142] Fractions were collected from each step of the immunoprecipitation experiment and were fractionated on a one-dimensional gel followed by western blot analysis for Ub (Figure 4.3). The gel had two bands in elution lane 9 at masses 25kDa and 50kDa. While the bands could be indicative of ubiquitinated proteins, it could also be the heavy and light chain on the antibody, since crosslinking of antibody to beads was not performed. Crosslinking of FK2 antibody has been shown to disrupt the antibodies ability to bind to Ub conjugates.[142] A light band at 75kDa was also observed, but at that mass, a top-down mass spectrometry analysis is not possible. The western blot analysis, performed with an anti-Ub antibody FK2, (Figure 4.3 b), showed bands below 25kDa in the flowthrough sample. This is indicative of the FK2 antibody immunoprecipitation not working, and the FK2 antibody not recognizing the Ub conjugates. Therefore, a strategy without purification of the Ub conjugates was attempted, even though the advantage of having a simplified mixture of protein to analyze on the HPLC will be lost.

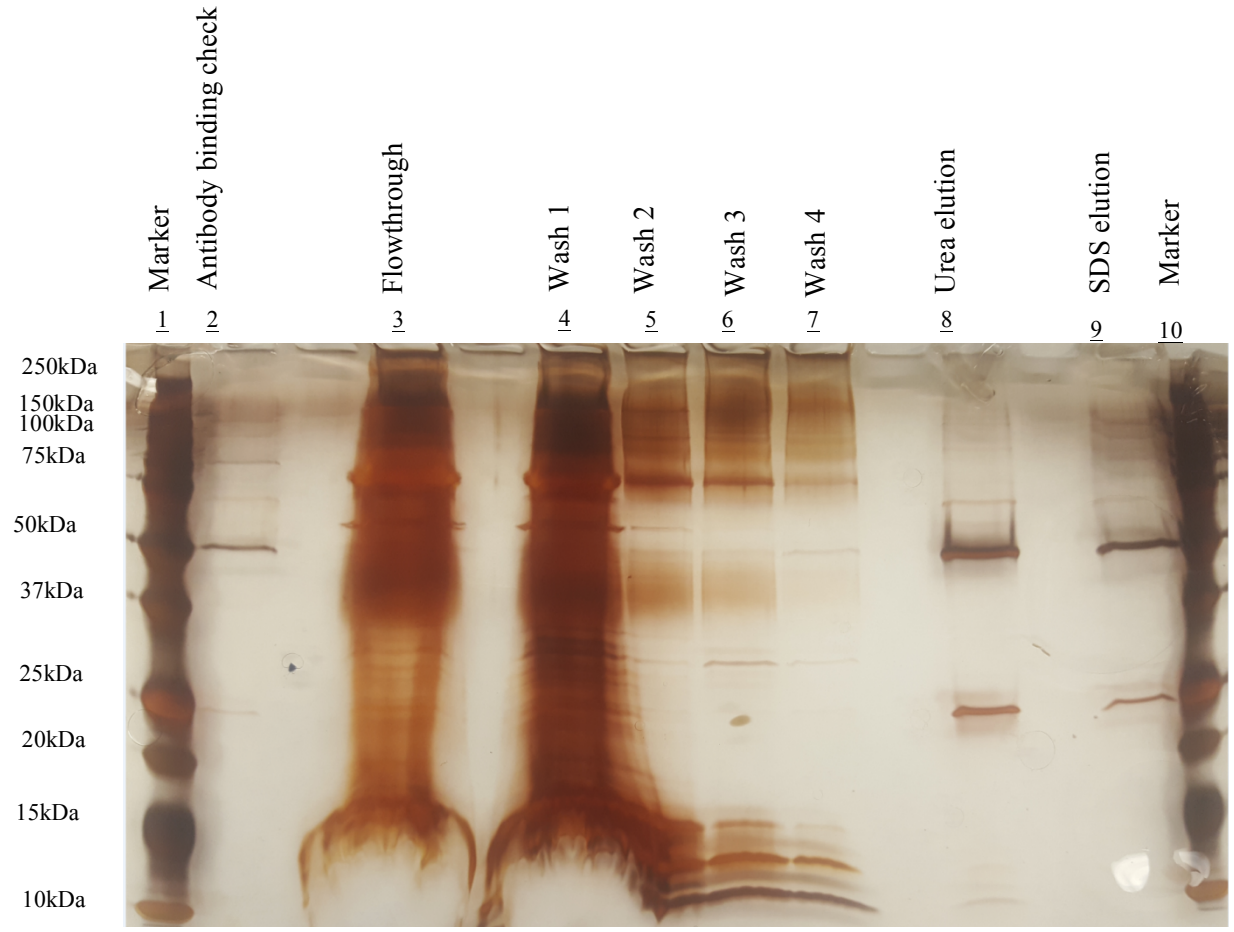
Marker
Antibody binding check
Flowthrough
Wash 1
Wash 2
Wash 3
Wash 4
Urea elution
SDS elution
Marker
1
2
3
4
5
6
7
8
9
10
250kDa
150kDa
100kDa
75kDa
50kDa
37kDa
25kDa
20kDa
15kDa
10kDa

**4.3A.**

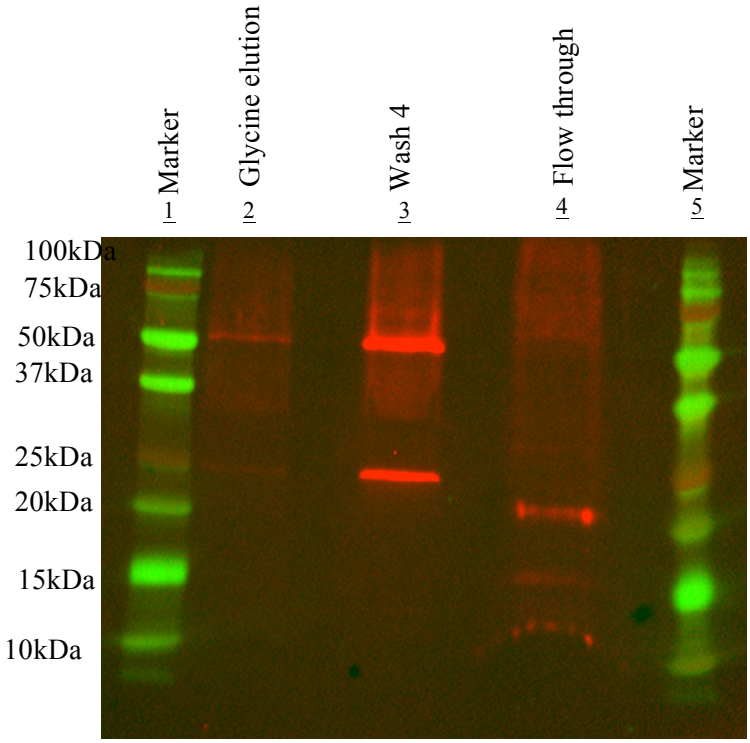
Marker
Glycine elution
Wash 4
Flow through
Marker
1
2
3
4
5
100kDa
75kDa
50kDa
37kDa
25kDa
20kDa
15kDa
10kDa

**4.3B.**

**Figure 4.3.** Fractions collected from the immunoprecipitation using the anti-Ub FK2 antibody run on. a one-dimensional gel, silver stained. B. run on a one dimensional gel followed by a western blot against Ub.

*4.3.3. Top down analysis of exosome proteins*

The protein cargo of exosomes was analyzed using top-down mass spectrometry without any enrichment of Ub conjugates or fractionation of the lysate. The precursor tolerance window was expanded to 40 kDa, using the bioinformatics program Prosight PD. A wide tolerance for the mass of the precursor ions would allow for the identification of polyubiquitin with a large addition of mass, which would occur if it were conjugated to a protein. Monoubiquitin was identified in the exosome lysate eluting at 74 min (Figure 4.4). Studies by Lee et al have shown the occurrence of fragmentation in the first 18 residues of Ub in top-down studies of synthetic Ub.[53] In our current study, fragmentation of the endogenous monoUb from exosomes is shown in Figure 4.5, which confirms the fragmentation of residues 1-18, as 9 out of the possible 18 c-ions are observed.

Figure 4.4 shows the extracted ion chromatogram for the precursor mass of monoUb followed by extracted ion chromatograms for expected product ions for c ions expected from the N-terminus of the monoUb. These ions are termed as the class characteristic ions of ubiquitin. Since ubiquitin can either attach from its lysine residues to other Ub or through its C-terminal residues to other substrate protein, the c/b-ions from the first 18 residues will be deterministic of the presence of ubiquitin. Ubiquitin conjugated to a substrate protein will not have the expected precursor mass of either Ub or the attached protein; therefore, looking for the class characteristic c-ions is a preliminary indicator of possible Ub conjugates. In our current top-down investigation of MDSC-derived exosomes, a series of class characteristic c- or b-ions was not observed at other retention times. Therefore, polyUb or Ub conjugated proteins have not been identified in exosomes using top-down mass spectrometry thus far using this method.

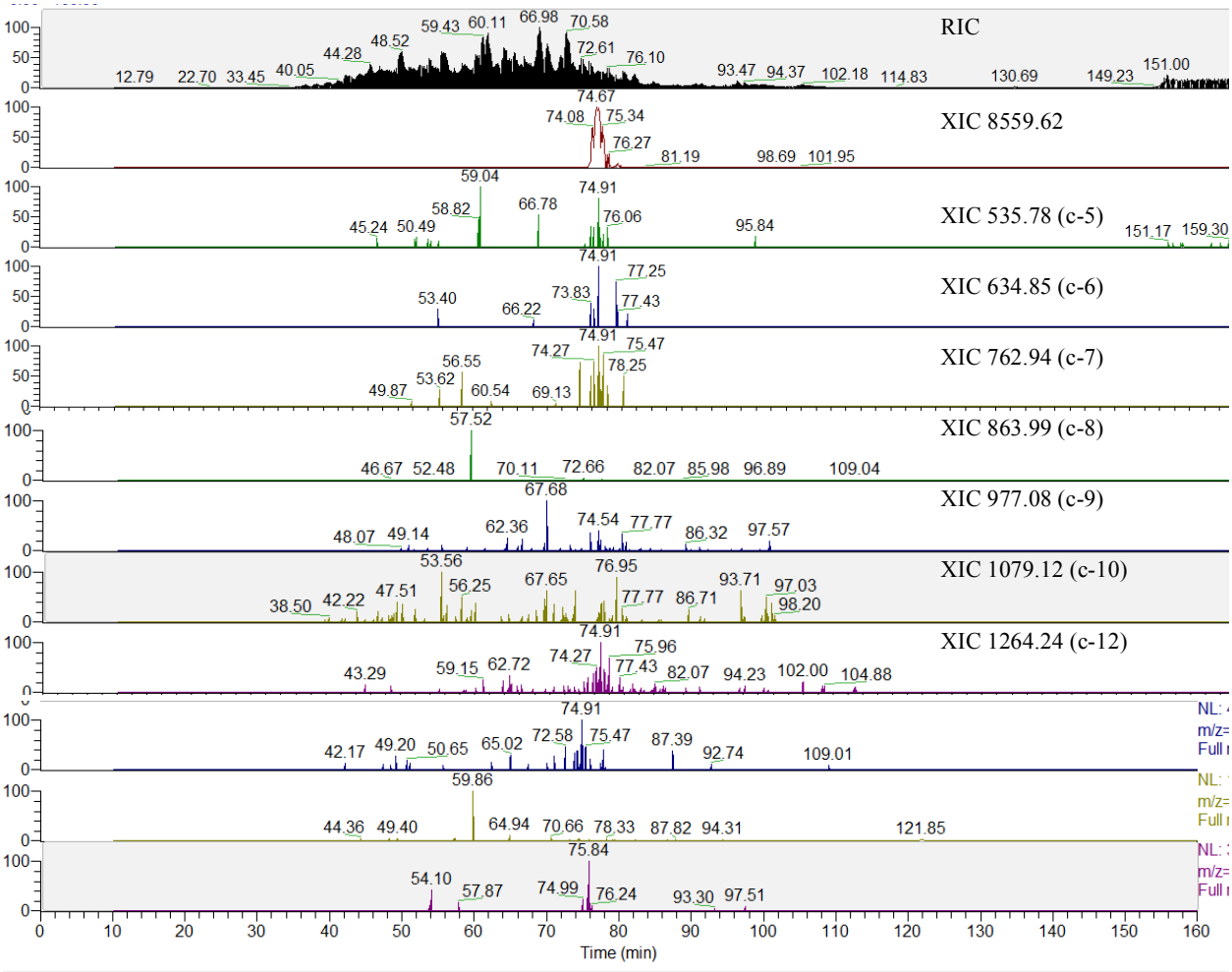


**Figure 4.4.** Reconstructed ion chromatogram (RIC) for exosome protein lysate top-down analysis and extracted ion chromatograms (XIC) for the monoisotopic mass of Ub (8559.62), and XIC of c-ions c-5 to c-13 of ubiquitin.

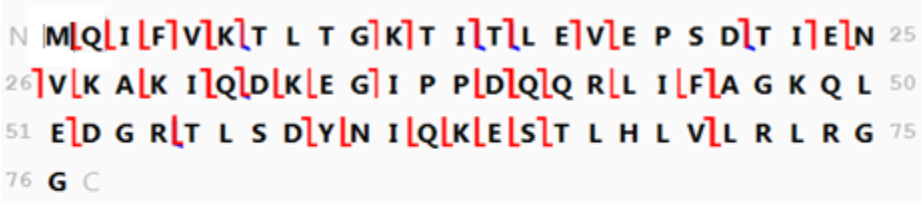


**Figure 4.5.** Sequence of a monoUb with c-, b-, y- and z-ions identified from the top-down analysis. The c- and z- ions are depicted by red carats and the b- and y-ions are depicted by blue carats.

The raw data for the top-down analysis of Ub exosomes was also processed using the Prosight software node in Proteome Discoverer with a wide window for precursor mass tolerance (40,000Da). This would allow us to identify proteins at unexpected masses, which would be the case with a protein with ubiquitin attached to it. A total of 29 proteins were identified based on fragmentation using top-down mass spectrometry from the MDSC-derived exosomes (Table 4.2). Forty-four percent of the proteins identified were from the histone family. The proteins highlighted in grey in Table 4.2 correspond to proteins also identified from the bottom-up analysis, which were listed in Table 4.1. Comparing the two tables shows that top-down and bottom-up are complementary approaches of analyzing a protein mixture. The top-down analysis yielded the identification of several histones, which were not identified in the bottom-up analysis and vice versa.

Most proteins identified were not identified at their expected molecular weights, but identified with smaller molecular weights. The only proteins identified at their expected molecular weights were ubiquitin, S100A8, and CDNA sequence BC100530 (an un-reviewed entry on Uniprot) (Appendix 4.1). Therefore, we conclude that exosomes are carrying many truncated proteins amongst their cargo of functional proteins. Ubiquitin was not identified with an increase in mass, which would have led to the possibility of identifying a Ub conjugate or a polyUb.

**Table 4.2.** Proteins identified in the top-down analysis of MDSC-derived exosomes. The proteins highlighted in grey were also identified in the bottom-up analysis and weighed less than 21.5 kDa (Table 4.1).

| Accession No | Protein Name |
|---|---|
| P60710 | Actin, cytoplasmic 1 |
| E9Q5F4 | Actin, cytoplasmic 2 |
| Q91Z25 | Actin-related protein 2/3 complex subunit 1B |
| Q91VB8 | Alpha globin 1 |
| Q497J0 | CDNA sequence BC100530 |
| G3UYK8 | Coronin |
| D3Z510 | Fructose-bisphosphate aldolase A |
| D3Z510 | Fructose-bisphosphate aldolase A |
| P62827 | GTP-binding nuclear protein Ran |
| Q61646 | Haptoglobin |
| P01942 | Hemoglobin subunit alpha |
| P02088 | Hemoglobin subunit beta-1 |
| P02089 | Hemoglobin subunit beta-2 |
| F8WIX8 | Histone H2A |
| P22752 | Histone H2A type 1-B |
| Q8CGP6 | Histone H2A type 1-H |
| P27661 | Histone H2AX |
| P70696 | Histone H2B type 1-A |
| Q64475 | Histone H2B type 1-B |
| Q6ZWY9 | Histone H2B type 1-C/E/G |
| P10853 | Histone H2B type 1-F/J/L |
| Q64478 | Histone H2B type 1-H |
| Q8CGP1 | Histone H2B type 1-K |
| P10854 | Histone H2B type 1-M |
| Q64525 | Histone H2B type 2-B |
| Q9D2U9 | Histone H2B type 3-A |
| O08692 | Neutrophilic granule protein |
| P0CG50 | Polyubiquitin-C |
| P27005 | Protein S100-A8 |
| A0A1L1SQV8 | Pyruvate kinase PKM |

An experiment with linear K-48 linked Ub trimer spiked into the MDSC-exosome lysate was performed. The standard was added at the following increasing concentrations- 1%, 2.5%, 5%, and 20% of the total exosomal protein content (Figure 4.6). The objective was

to check the signal intensity of a polyUb at different concentrations in a complex protein lysate, since we were concerned about the lack of evidence of Ub conjugates using top-down mass spectrometry. The results in Figure 4.6 indicate that even at low levels of unanchored polyUb, our instrument and methods employed for the LC-MS/MS analysis are successful at identifying the mass of Ub trimer. It is also apparent that with increasing concentration of Ub trimer in the MDSC-exosome lysate, the normalized signal intensity (NL) also increases (Figure 4.6). However, good fragmentation is required to make identifications based on class characteristic ions and Prosight PD. Figure 4.7 shows the fragmentation patterns for the Ub trimer added in various concentrations. Even though molecular ions for the Ub trimer could be detected at 1% concentration, the fragment ions are not strong enough to identify the precursor as a Ub trimer. At 2.5% and 5% only one fragment (b- and c-ions 218) shows proof of polyUb. It is not until we get to 20% concentration of polyUb in the exosome lysate that we observe several fragments, which are specific for a polyUb chain.

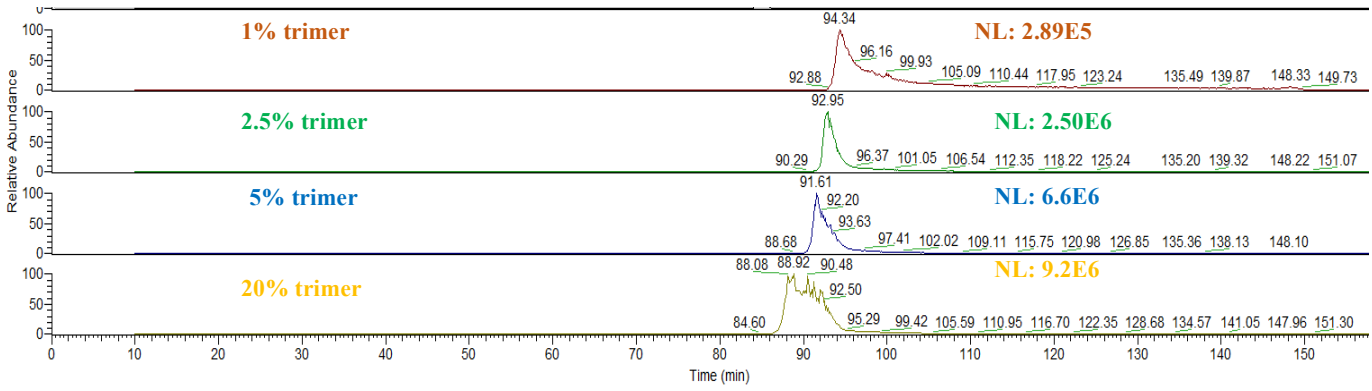


**Figure 4.6**. Extracted ion chromatograms of mass-25657.50 Da from the spike in experiments at different concentrations of K-48 linked Ub trimer in MDSC-exosome protein lysate.


**Figure 4.7.** Fragment c-,z-,b- and y-ions identified from K-48 linked linear Ub trimer spike-in experiments in exosome protein lysates.

*4.4. Conclusions*

Purification techniques used to enrich for Ub conjugate from the protein lysates of MDSC-derived exosomes were not successful. The agarose-TUBES were specific for poly-Ub conjugates and unanchored polyUb, and perhaps the MDSC exosomes do carry a higher concentration of monoUb and multiple mono-Ub conjugates. The anti-Ub FK2 antibody was not successful in isolating Ub conjugated proteins as evidenced by bands observed in western blots of the flow through fraction of the immunoprecipitation experiment. Finally, the top-down analysis of the non-enriched lysate of MDSC-derived exosomes identified mono-Ub but failed to identify unanchored polyUb or Ub conjugated proteins. This could be a result of the exosomes carrying long chains of polyUb or multiple mono-Ub conjugates, which will not be in the detectable mass range of the mass spectrometer. This hypothesis is validated by the finding that a large concentration of a polyUb trimer (26 kDa) is required for acquiring fragmentation to confirm the presence of a trimer. It is unrealistic to expect a polyUb conjugate to make up 20% of the total protein concentration, as would be required for identification of a polyUb. Therefore, in order for the strategy involving class characteristic ion fragmentation to work, narrower, and higher HPLC peaks will be required. Also, with our current capabilities, 200 ng of a polyUb trimer will be required for attaining fragmentation to discern the presence of a Ub trimer. The same holds true for the identification of polyUb using Prosight PD which also requires fragmentation to identify proteins.

# Chapter 5: Conclusions and future prospectus

Myeloid derived suppressor cells (MDSC) are immunosuppressive cells present in most cancer patients.[143] These cells are known to release exosomes into the tumor microenvironment, and these exosomes have been found to contain biologically active molecules.[7,19,128] The presence of MDSC in the body leads to suppression of adaptive and innate immune responses, and poses a hurdle for successful immunotherapy. The exosomes shed by MDSC have also been shown to carry proteins that use chemotactic activity to lead to the accumulation of the parental cells, which increases the potency of the immunosuppressive function.[7,128]

The work presented in this thesis focuses on interrogating the protein cargo carried by the MDSC derived exosomes, in an effort to gain insights on the mechanisms of their immune suppression and intercellular communication. Post-translational modifications can determine protein function and cellular interactions. Therefore, this study exploited PTM's to enrich proteins carried by MDSC exosomes that may be lower in abundance or difficult to identify in a shotgun proteomic approach.

First, a method to identify exosomal surface glycoproteins was successfully employed. It was determined that the surface of the exosomes closely resembles that of the parental cells. Many of the identified surface molecules on the exosomes had the potential to regulate activity and function of the parental cells. Amongst these molecules the strongest case was made for CD47, as it was demonstrated that exosomal CD47 enhanced the accumulation of the MDSC, thereby increasing immunosuppressive activity.

The second objective was to interrogate the PTM of ubiquitination using bottom-up proteomics. It was determined that the exosomes were carrying a highly ubiquitinated cargo of proteins. Bioassays demonstrated that some of the ubiquitinated proteins carried by the

MDSC derived exosomes can play a role in MDSC chemotaxis. The presence of enzymes involved in the conjugation of Ub, and enzymes involved in the production of ATP, led to the hypothesis that ubiquitination could occur *in situ* in MDSC- derived exosomes.

Exosome cargo was also examined using a top-down proteomic strategy, which revealed that many proteins are present in multiple truncated proteoforms. This is consistent with an older idea that exosomes remove "junk" cellular debris (including proteins) from cells. It is also consistent that proteasome activity has been demonstrated in exosomes. No ubiquitinated conjugates were characterized, but it is possible that they are larger than 30kDa, which is the current limit of detection of top-down mass spectrometry.

Future biological assays on proteins identified on the surface and also on selected ubiquitin conjugates would continue to define the biological relevance of the protein cargo. The studies performed in this thesis homed in on the effects of the exosomal protein cargo on the parental cells.[144] However, it would be of interest to test the role of MDSC-exosomal surface proteins in communicating with other cellular players in the complex tumor microenvironment. The top-down strategy to evaluate ubiquitinated protein cargo has great potential for future development. Implementing a successful strategy to fractionate the exosomal protein cargo, with sharper peaks in liquid chromatography time-scale would help in identification of larger ubiquitinated protein complexes. Optimization of the fragmentation method used in the mass spectrometer would also be required. Also, bioinformatics software currently does not have the capability to identify truncated ubiquitinated proteins. The lack of bioinformatics tools will be a challenge since many truncated proteins were identified in the exosomal cargo. However, with optimized MS2 fragmentation, characteristic b-ions can be used to recognize and short-list precursor ions of ubiquinated proteins. The spectra identified could then be interpreted using a combination of bioinformatics tools such as Prosight PC and Prosight PD.